Coupling Reactions Using Excited State Organonickel Complex

171118_LS_Daiki_Kamakura

Ni Catalysis in Coupling Reactions

9	10	11
Co	$_{28}$Ni	Cu
Rh	Pd	Ag
Ir	Pt	Au

Features of Ni

- **d electrons: 8**
- **relatively inexpensive (Ni: $1/g, Pd: $183/g, Pt: $483/g)**
- **easier accessibility of $Ni^0/Ni^I/Ni^{II}/Ni^{III}/Ni^{IV}$ oxidation states**

Coupling reactions using Ni catalysis

coupling with nucleophile

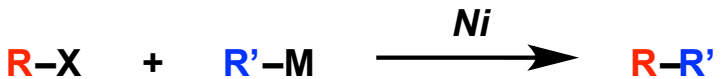

R = sp^3, sp^2

X = Cl. Br, I, OTf, OMe, OH…

coupling with electrophile

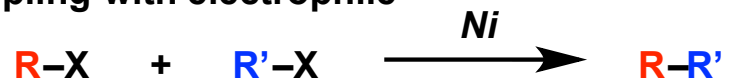

R' = sp^3, sp^2, sp, NR_2, OR, OH

M = BR_2, MgX, ZnX, SiX_3

C-H activation

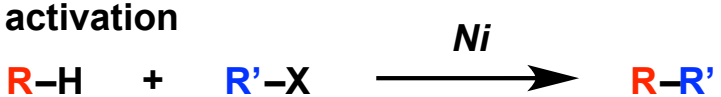

In all of these reactions, ground state Ni complex was used.
So excited-state metal catalysts remains largely unexploited.

Netherton, M. R., Fu, G. C. *Adv. Synth. Catal*. **2004**, *346*,1525.
Tasker, S. Z., Standley, E. A., Jamison, T. F. *Nature*, **2014**, *509*, 299 .
Su, B., Cao, Z-C., Shi, Z-J. *Acc*, *Chem Res*, **2015**, *48*, 886.
Ananikov, V. P. *ACS Catal*. **2015**, *5*, 1964.

Photo Reactions of Metal Complex

Classical reactions

ligand elimination

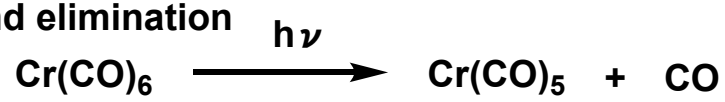

ligand exchange

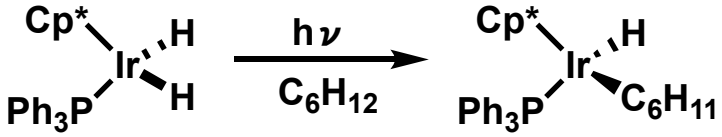

Janowicz , A. H., Bergman, R. G. *J. Am. Chem. Soc*, **1983**, *105*, 3930.

Recently reported chlorine photoelimination

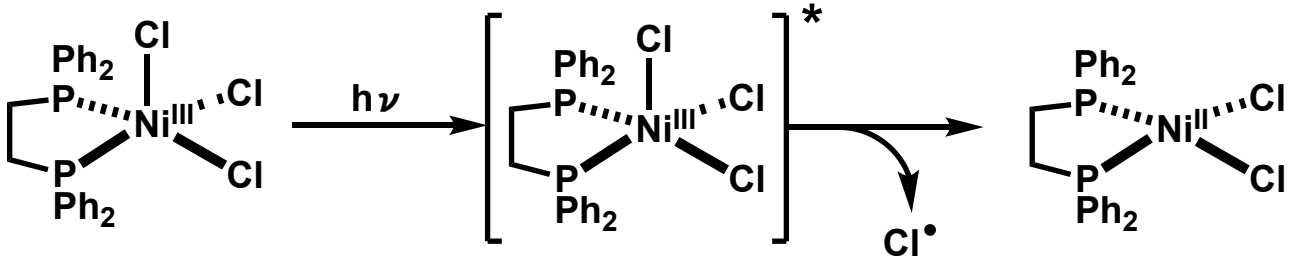

Hwang, S. J., Powers, D. C. Maher, A. G., Anderson, B. L., Hadt, R. G., Zheng, S-L., Chen, Y-S., Nocera, D. G. *J. Am. Chem. Soc*, **2015**, *137*, 6472

Contents

Contents

C-H Functionalization of Amines with Aryl Halides

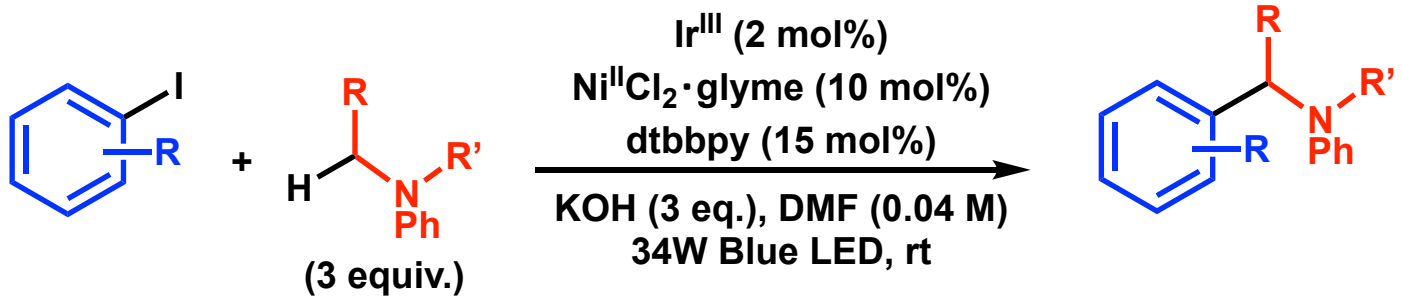

Proposed mechanism

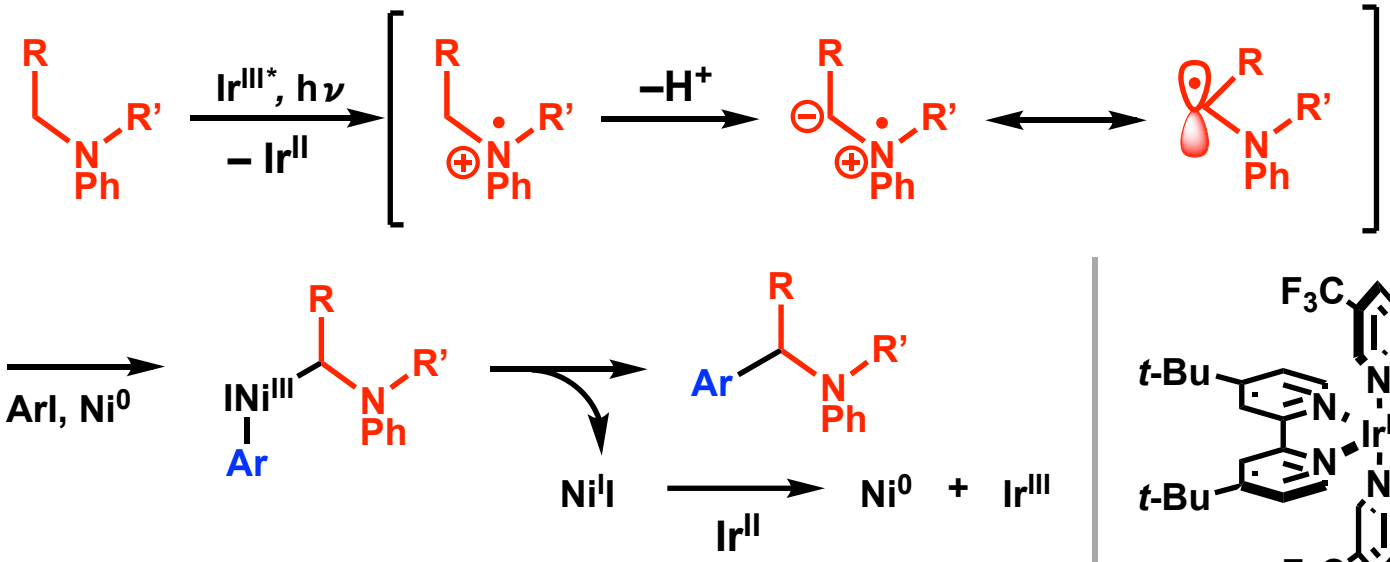

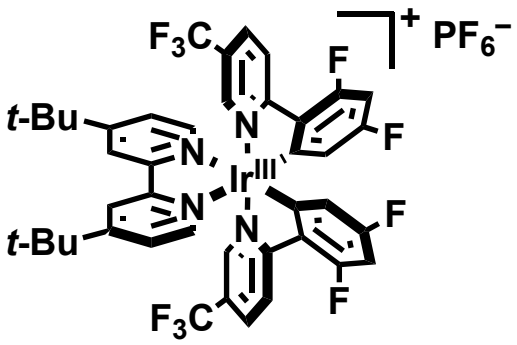

Ir^III = [Ir^III(dF-CF3-ppy)2(dtbpy)]PF6

Ahneman, D. T., Doyle, A. G. *Chem. Sci*, **2016**, *7*, 7002.

Difficulty of Application for α-Arylation of Ether

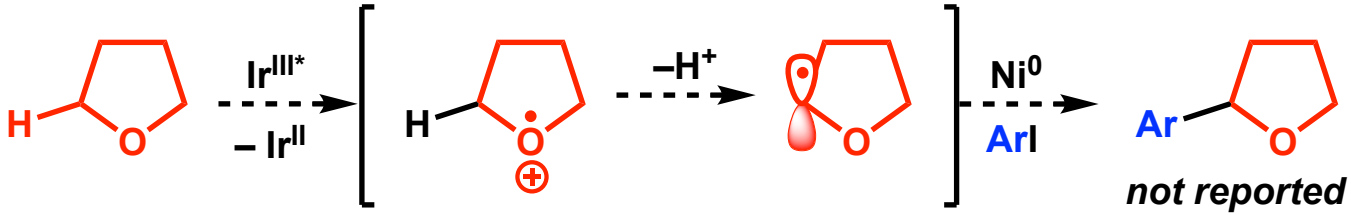

not reported

$E_1/_2$ (Ir^{III*}/Ir^{II}) = 1.21 V

$E_1/_2$ ($THF^{\cdot+}$/THF) = 1.75 V

Oxidation of THF: *disfavored* (ΔE = –0.69 V)

$E_1/_2$ ($PhR_2N^{\cdot+}/PhR_2N$) = 0.70 V
R = $–(CH_2)_4–$

Oxidation of Amine: *favored* (ΔE = 0.51 V)

Usage of more storong oxidant

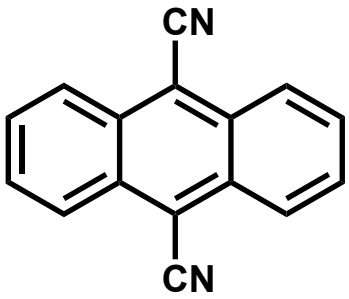

DCA

$E_1/_2$ ($DCA^*/DCA^{\cdot-}$) = 2.07 V

Oxidation of THF: *favored* (ΔE= 0.32 V)

$E_1/_2$ (Ni^I/Ni^0) = –1.2 V

$E_1/_2$ ($DCA/DCA^{\cdot-}$) = –1.01 V

$E_1/_2$ (Ir^{III}/Ir^{II}) = –1.37 V

Reduction of Ni^I by $DCA^{\cdot-}$
: *disfavored* (ΔE= –0.2 V)

Reduction of Ni^I by Ir^{II}
: *favored* (ΔE= 0.36 V)

Ir^{III} = $[Ir^{III}(dF\text{-}CF_3\text{-}ppy)_2(dtbpy)]PF_6$, Ni^I = $(dtbpy)Ni^IBr$

$A^+ + e^\ominus \longrightarrow A$ $\quad E_1/_2$ (A^+/A) = xx V

$B^+ + e^\ominus \longrightarrow B$ $\quad E_1/_2$ (B^+/B) = yy V

$A^+ + B \longrightarrow A + B^+$ $\quad \Delta E$ = (xx–yy) V

$\Delta G = –F\Delta E$

F: Faraday constant

$\Delta E>0 \longrightarrow \Delta G<0$

ΔE = 0.1 V ≈ ΔG = –2.3kcal/mol

Doyle's Working Hypothesis for α-Arylation of Ether

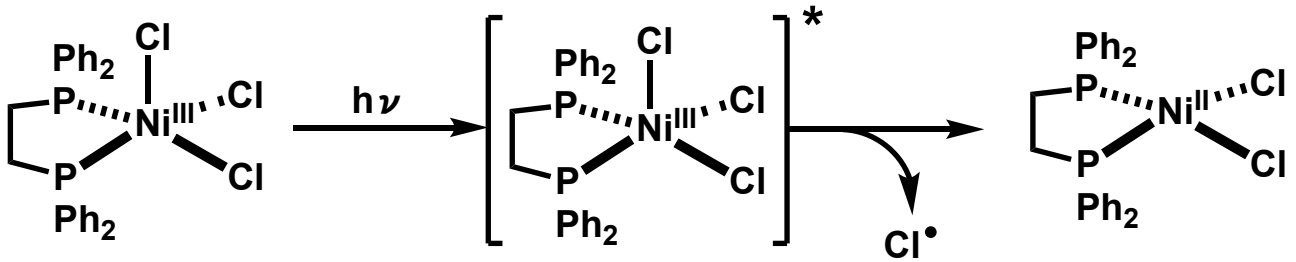

Hwang, S. J., Powers, D. C. Maher, A. G., Anderson, B. L., Hadt, R. G., Zheng, S-L., Chen, Y-S., Nocera, D. G. *J. Am. Chem. Soc*, **2015**, *137*, 6472

Doyle's Working Hypothesis

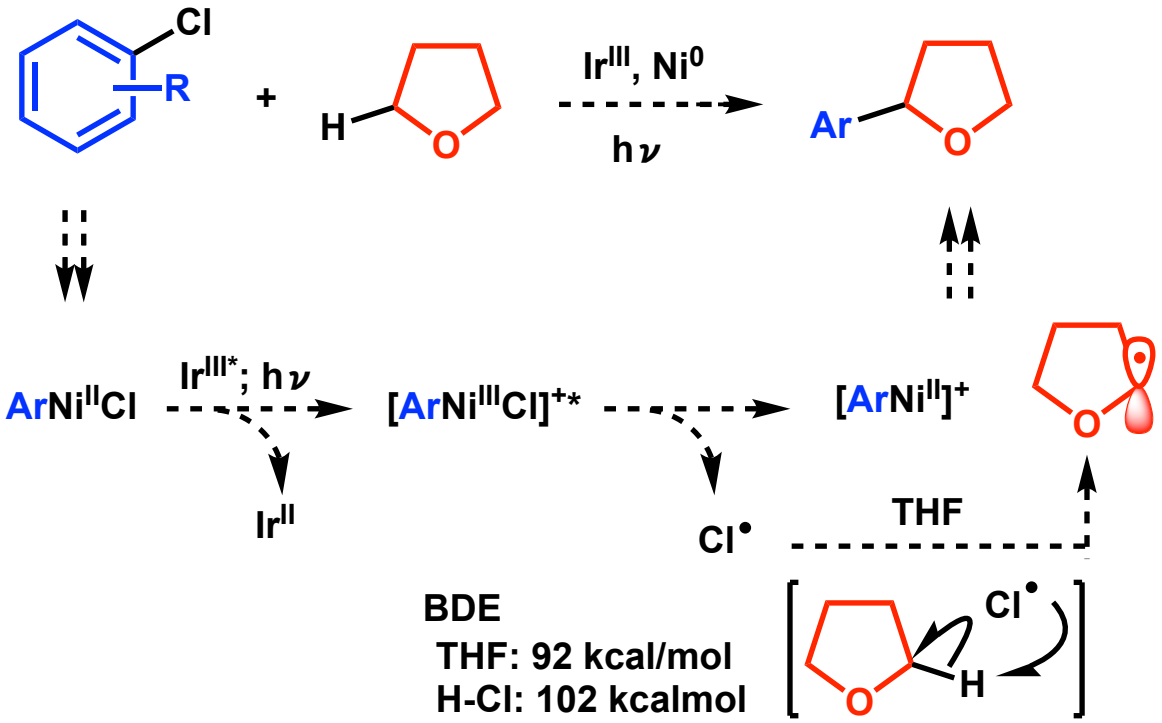

Shieds, B. J., Doyle, A. G. *J. Am. Chem. Soc.* **2016**, *138*, 12722

Optimization of THF α-Arylation Reaction

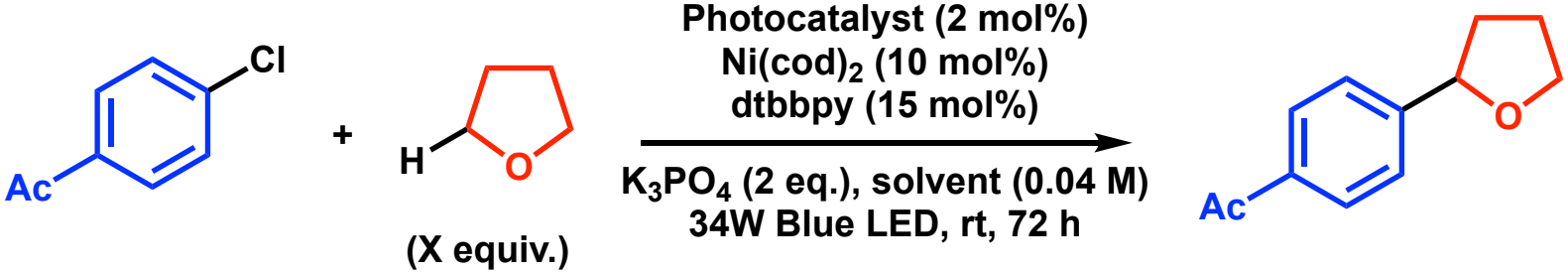

entry	photocatalyst	THF (X equiv.)	solvent	yield
1	$[Ir^{III}(dF\text{-}CF_3\text{-}ppy)_2(dtbpy)]PF_6$	1	benzene	20
2	$[Ir^{III}(dF\text{-}CF_3\text{-}ppy)_2(dtbpy)]PF_6$	10	benzene	71
3	$[Ir^{III}(dF\text{-}CF_3\text{-}ppy)_2(dtbpy)]PF_6$	THF (0.04 M)		92
4	none	THF (0.04 M)		0
5[a]	$[Ir^{III}(dF\text{-}CF_3\text{-}ppy)_2(dtbpy)]PF_6$	THF (0.04 M)		0
6[b]	$[Ir^{III}(dF\text{-}CF_3\text{-}ppy)_2(dtbpy)]PF_6$	THF (0.04 M)		0

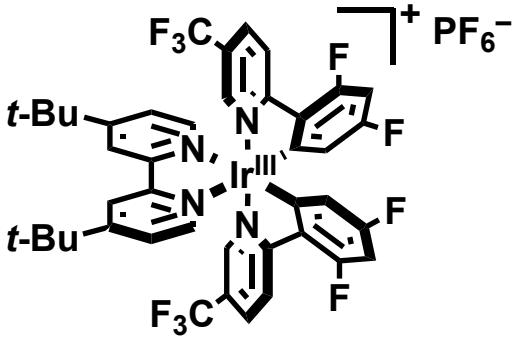

$[Ir^{III}(dF\text{-}CF_3\text{-}ppy)_2(dtbpy)]PF_6$

[a] $Ni(cod)_2$ was not added. [b] Reaction was conducted in the dark.

Shieds, B. J., Doyle, A. G. *J. Am. Chem. Soc.* **2016**, *138*, 12722

Sutoichiometric Oxidation Experiment

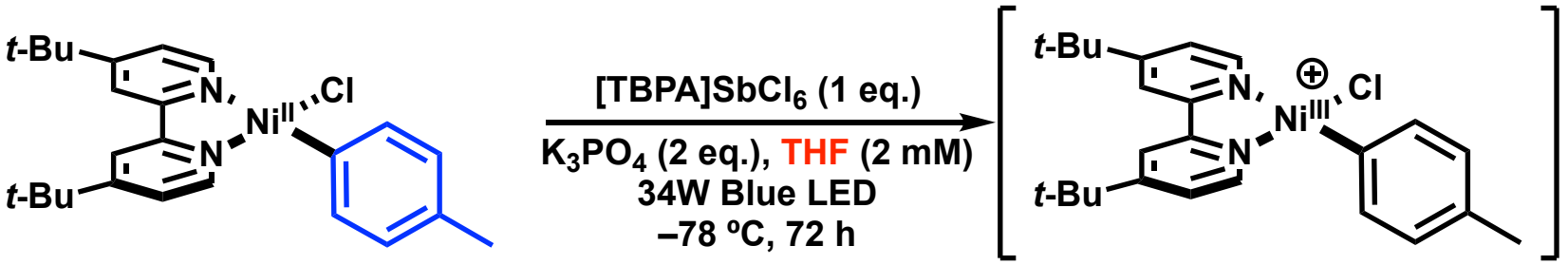

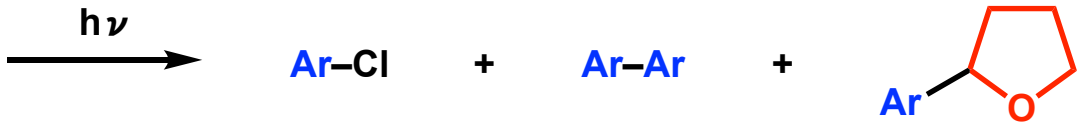

entry	*conditions*	Ar–Cl	Ar-Ar	Ar–THF
1	see above	6%	32%	20%
2	no oxidant	3%	62%	0%
3	dark	63%	9%	0%

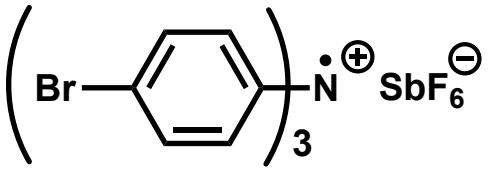

[TBPA]$SbCl_6$

$E_1/_2$ ($Ar_3N^{\cdot+}/Ar_3N$) = 1.16 V

$E_1/_2$ (Ni^{III}/Ni^{II}) = 0.85 V

Ni^{II} = (tbbpy)Ni^{II}(tol)Cl

Shieds, B. J., Doyle, A. G. *J. Am. Chem. Soc.* **2016**, *138*, 12722

Reactivity of Aryl Halides

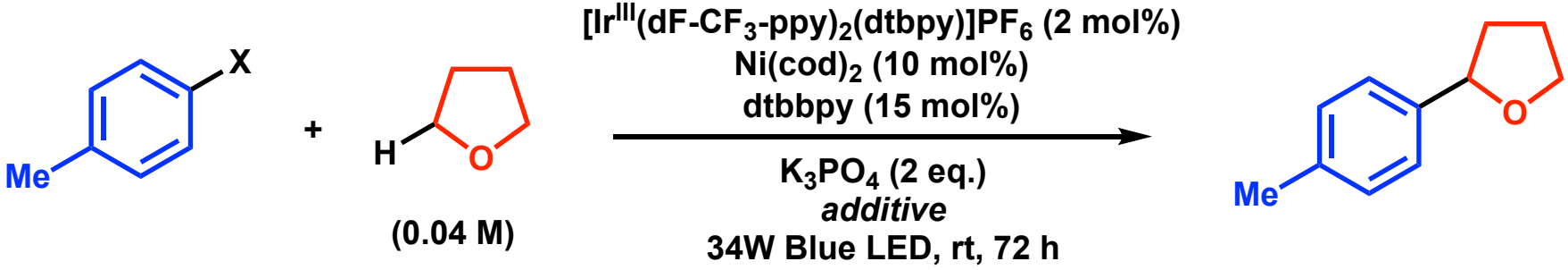

entry	X	*additive*	yield
1	Cl	none	68%
2	Br	none	10%
3	I	none	5%
4	I	TBAC	51%
5	I	TBAI	6%

TBA: tetrabutylammonium

BDE
THF: 92 kcal/mol
H–Cl: 102 kcalmol
H–Br: 87 kcal/mol
H–I: 71 kcal/mol

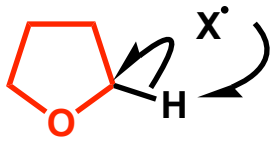

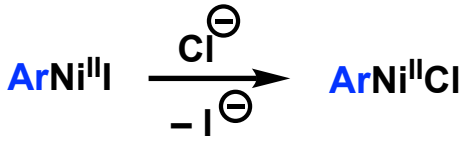

Shieds, B. J., Doyle, A. G. *J. Am. Chem. Soc.* **2016**, *138*, 12722

Proposed Catalytic Cycle

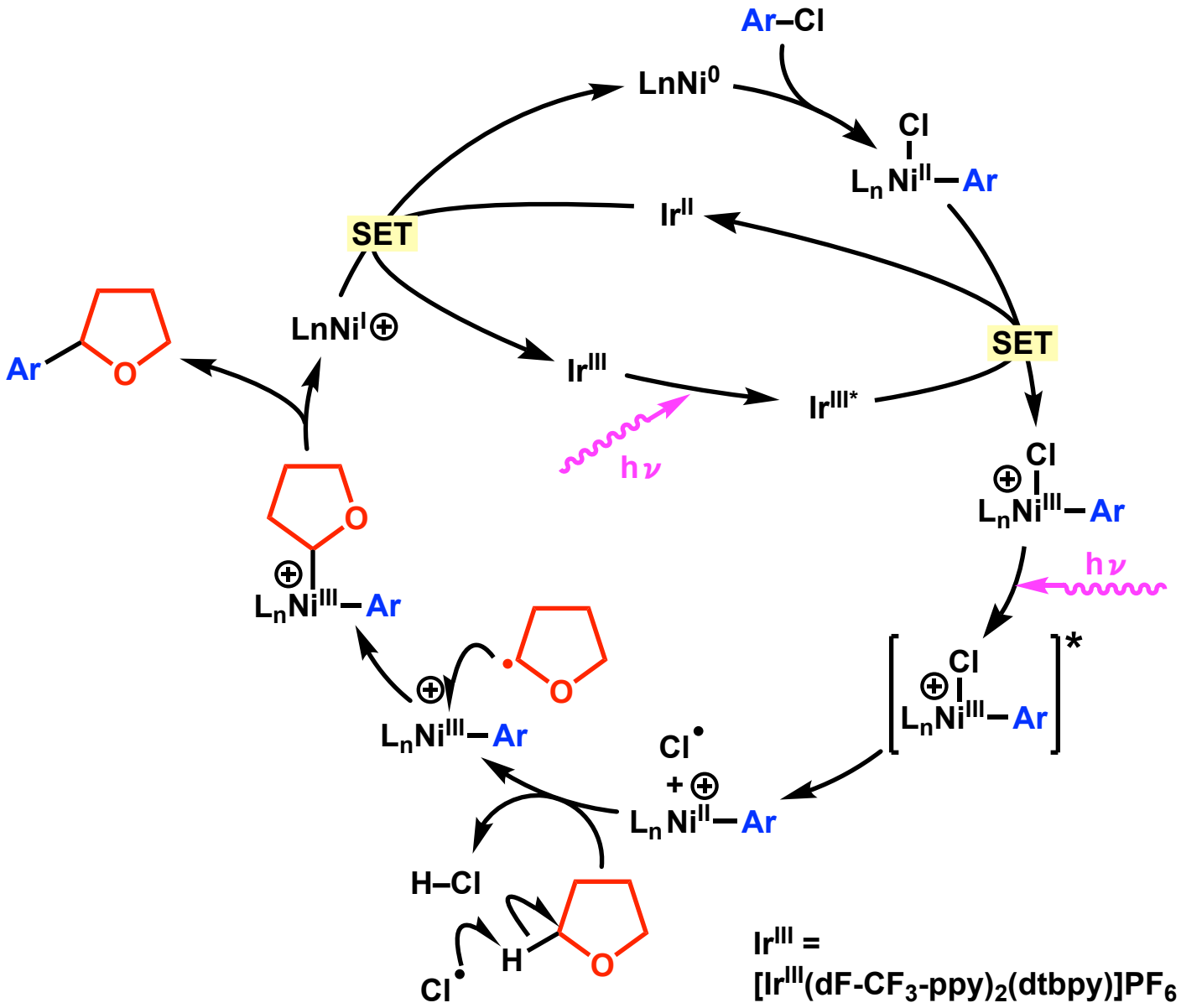

Shieds, B. J., Doyle, A. G. *J. Am. Chem. Soc.* **2016**, *138*, 12722

Substrate Scope of Aryl Chloride

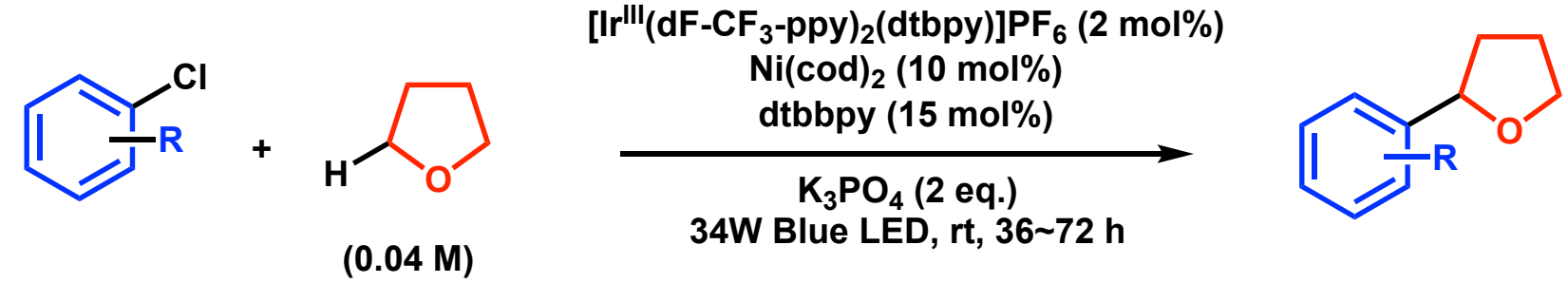

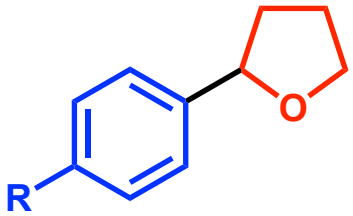

R = Me: 70%
R = Ph: 86%
R = OPh: 77%
R = CN: 83%
R = Ac: 79%
R = Bz: 76%

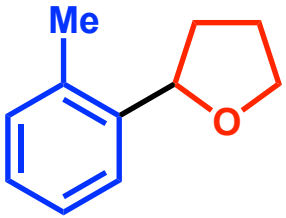

51%

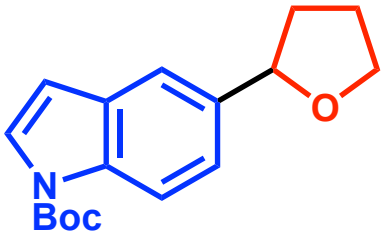

69%

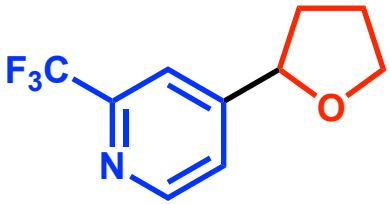

78%

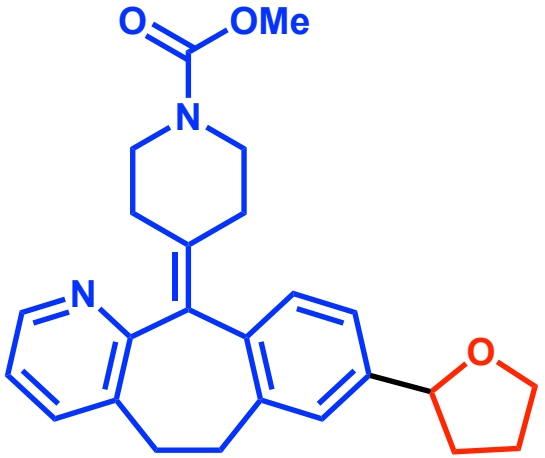

93%

Shieds, B. J., Doyle, A. G. *J. Am. Chem. Soc.* **2016**, *138*, 12722

Substrate Scope of Ether and Hydrocarbon

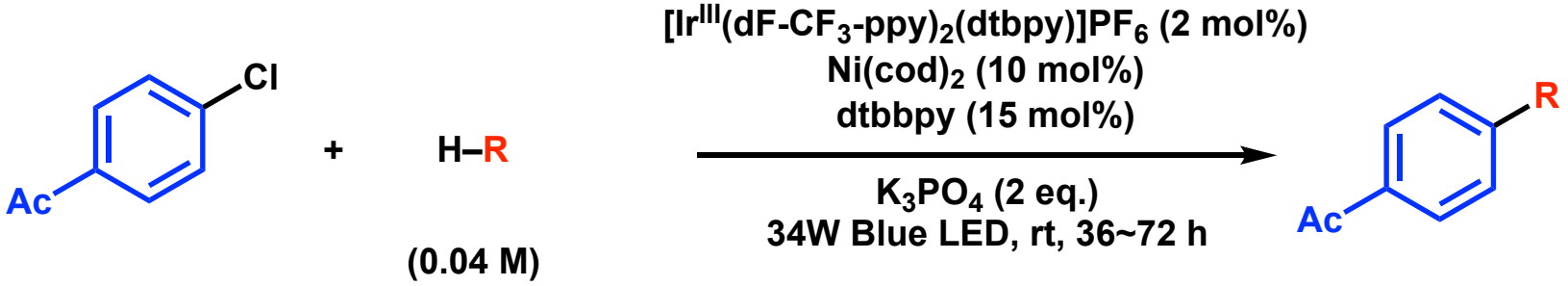

ether

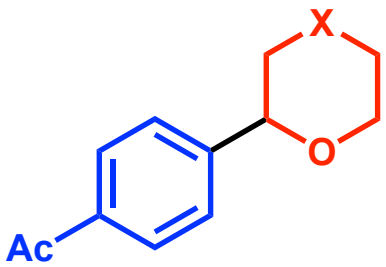

X = CH_2: 58%
X = O: 78%

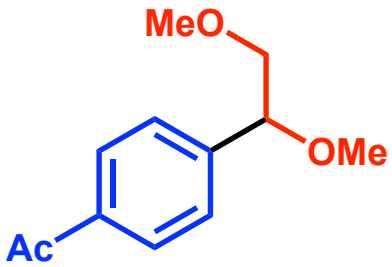

91%
(branch: linear = 1.35 : 1)

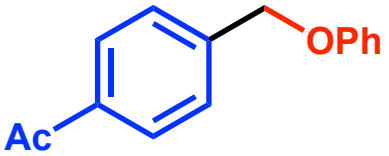

47%

hydrocarbon

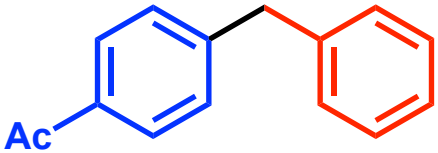

71%

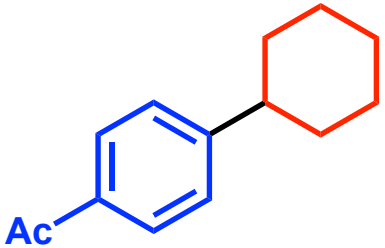

41%[a]

[a] 10 eq. of cyclohexane was used. Reaction was conducted in benzene (0.04 M).

Shieds, B. J., Doyle, A. G. *J. Am. Chem. Soc.* **2016**, *138*, 12722

Computational Studies

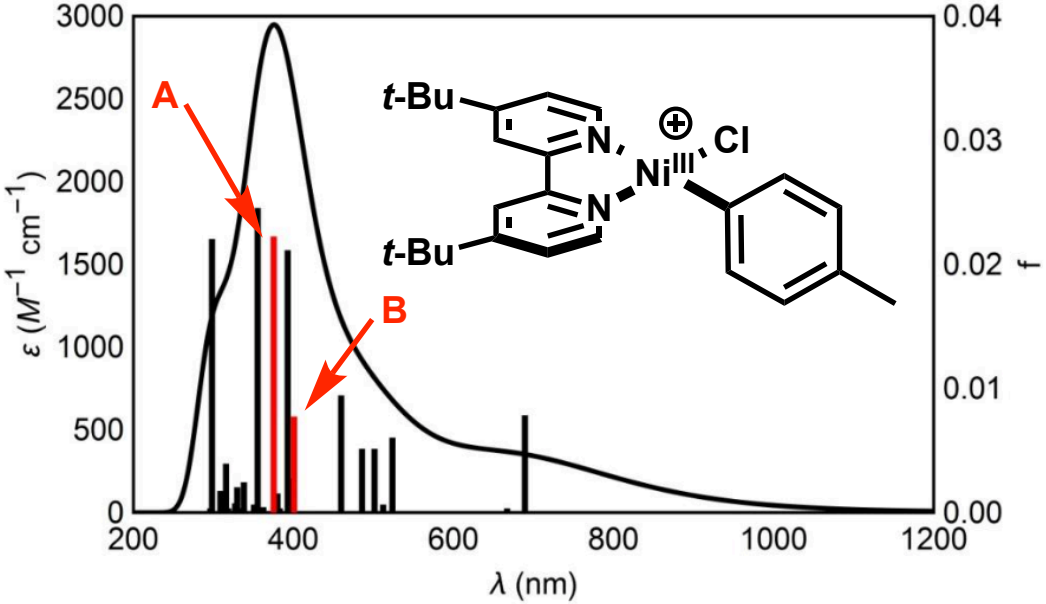

Fig. 1. Calculated absorption spectrum (solid black line) and oscillators (solid bars; red bars: transitions with > 10% Ni–Cl, σ → σ* contributions) from TD-DFT calculations on [Ni^{III}(dtbbpy)(Ph)Cl]$^+$.

transitions with > 10% Ni–Cl, σ → σ* contributions: A: 375, B: 401 nm

reaction was conducted under blue LED (λ>400 nm) so transition B would raise Ni–Cl dissociation

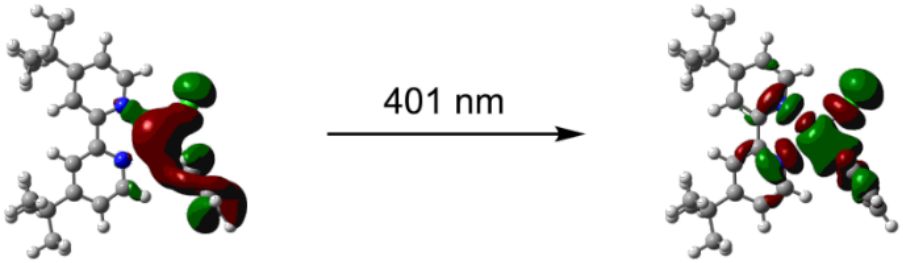

Fig. 2. Transition orbitals for excited state B of [Ni(dtbbpy)(Ph)Cl]+ (This transition has a large Ni–Cl σ → σ* component).

calc. BDE of [(dtbpy)(tol)Ni^{III}–Cl]$^+$: 56 kcal/mol

Ni–Cl could be cleaved by transition B (401 nm —> 71 kcal/mol)

Shields, B. J., Doyle, A. G. *J. Am. Chem. Soc.* **2016**, *138*, 12722

For all calculations the B3LYP hybrid exchange-correlation functional was used. Gas-phase geometry optimization and frequency calculations were carried out using a SDD basis set for Ni and Cl and 6-31G* for all other atoms.

Short Summary

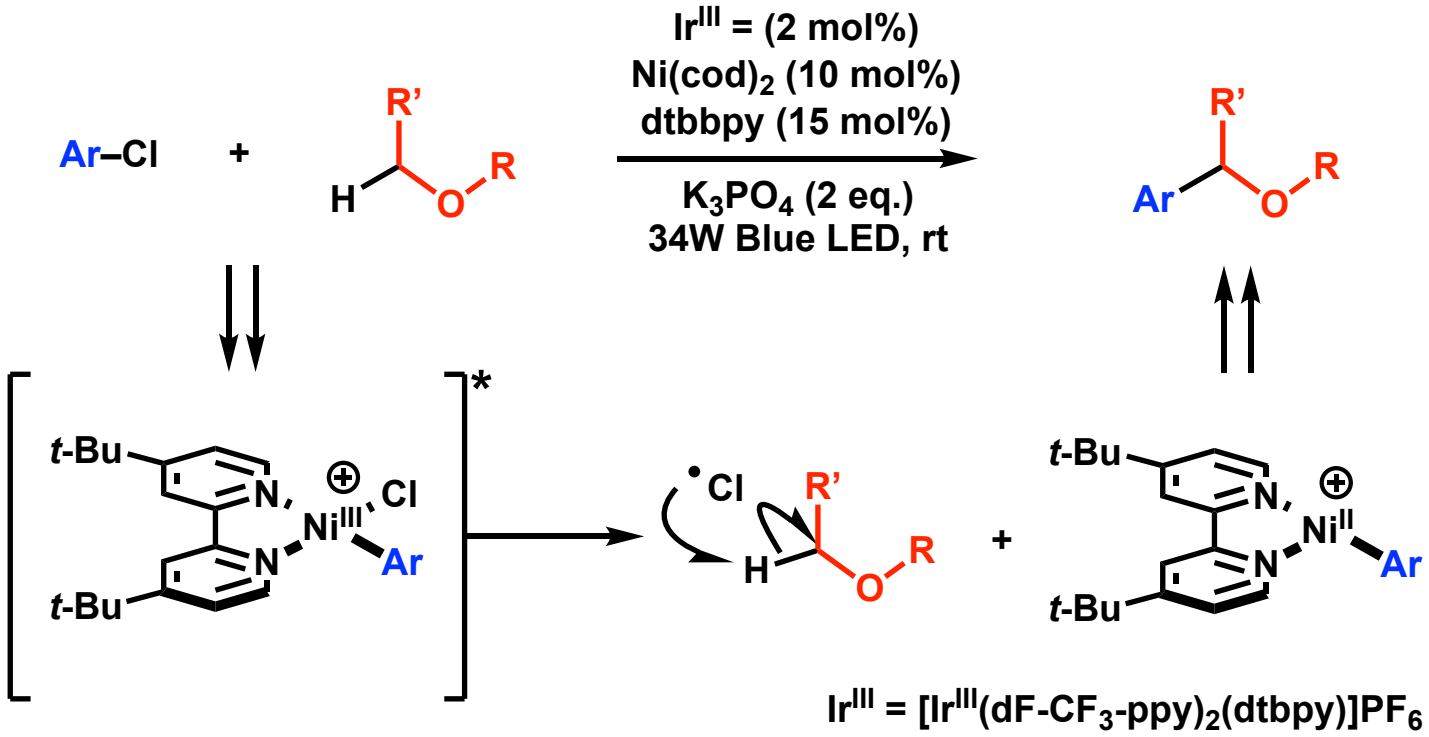

Shieds, B. J., Doyle, A. G. *J. Am. Chem. Soc.* **2016**, *138*, 12722

Contents

Coupling of Aryl Halide with Oxygen Nucleophiles

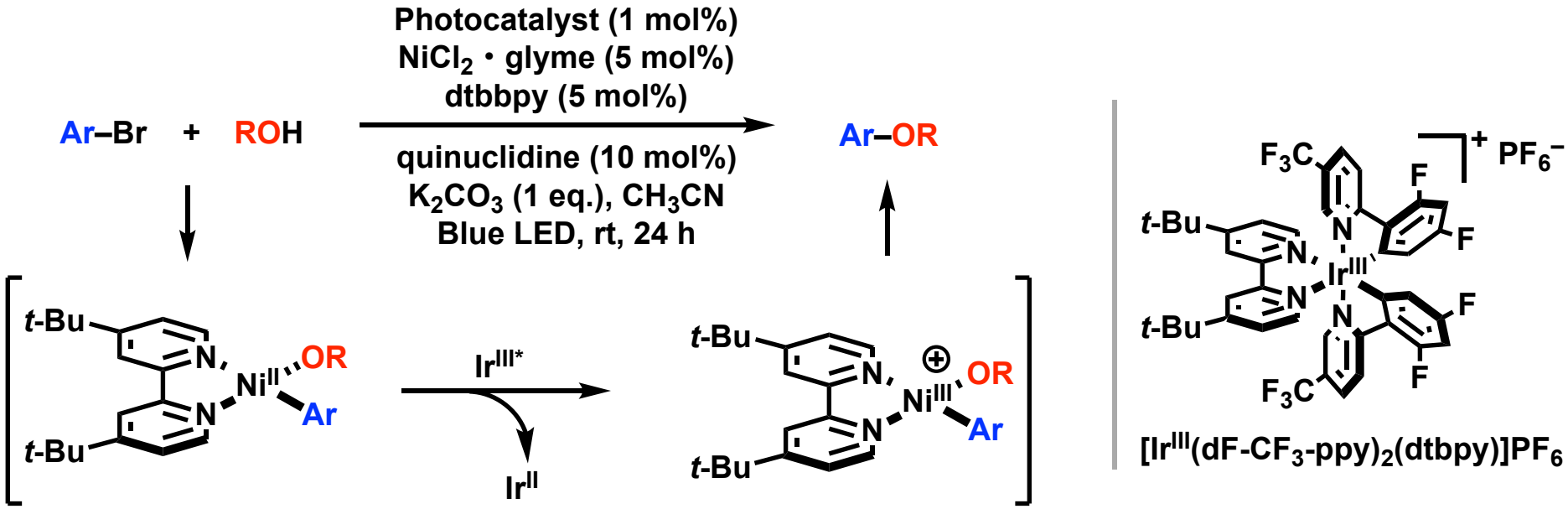

Terrett, J. A., Cuthbertson, J. D., Shurtleft, V. W., MacMillan, D. W. C. *Nature*, **2015**, *524*, 330.

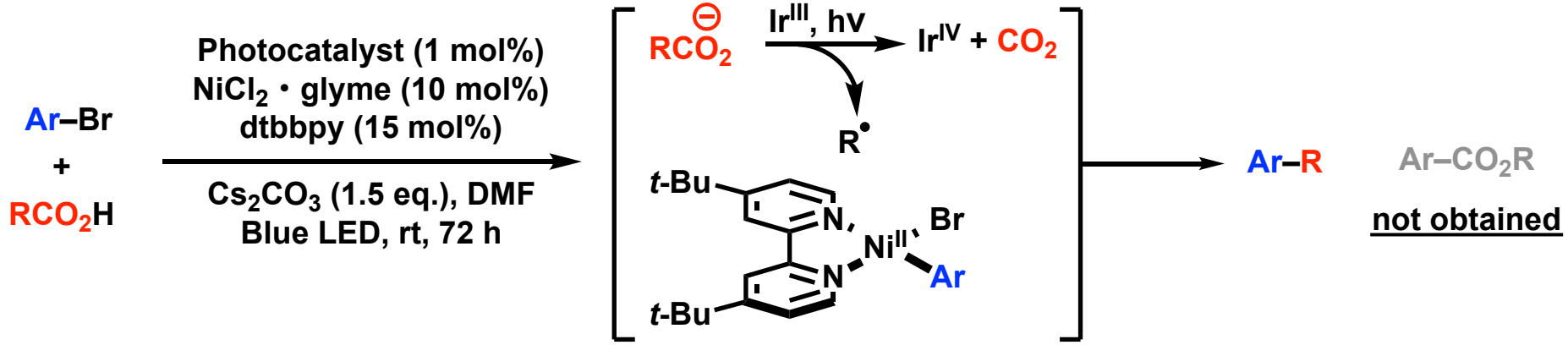

Zuo, Z., Ahneman, D. T., Chu, L., Terrett, J. A., Doyle, A. G. Macmillan, D. W. C. *Science*, **2014**, *6195*, 437.

Difficulty of Coupling Reaction with carboxylic Acid

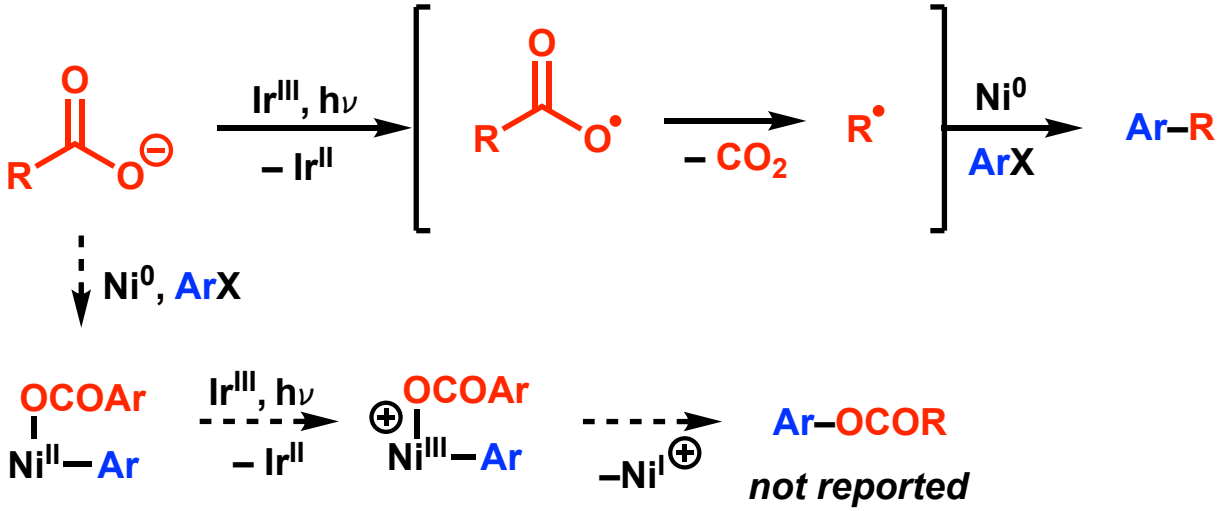

$E_1/_2$ (Ir^{III*}/Ir^{II}) = 1.21 V

$E_1/_2$ ($RCO_2^{\cdot}/RCO_2Cs$) = 0.95 V

$E_1/_2$ (Ni^{III}/Ni^{II}) = 1.00 V

Oxidation of RCO_2Cs: *favored* (ΔE = 0.26 V)

Oxidation of Ni^{II}: *favored* (ΔE = 0.21 V)

Ir^{III} = $[Ir^{III}(dF\text{-}CF_3\text{-}ppy)_2(dtbpy)]PF_6$

RCO_2Cs = Boc–Pro–OCs

⇨ Ni^{II} is exists only catalytic ammount so selective oxidation of Ni^{II} complex would be difficult

To surpless oxidation of carboxilic acid, usage of weaker oxidant is necessary,
but it makes difficult to oxidize Ni^{II} to Ni^{III}.

Welin, E. R., Le. C., Arias, R. D. M., McCusker, J. K., MacMillan, D. W. C. *Science*, **2017**, *355*, 380,

Coupling of Aryl Bromide with Carboxylic Acid

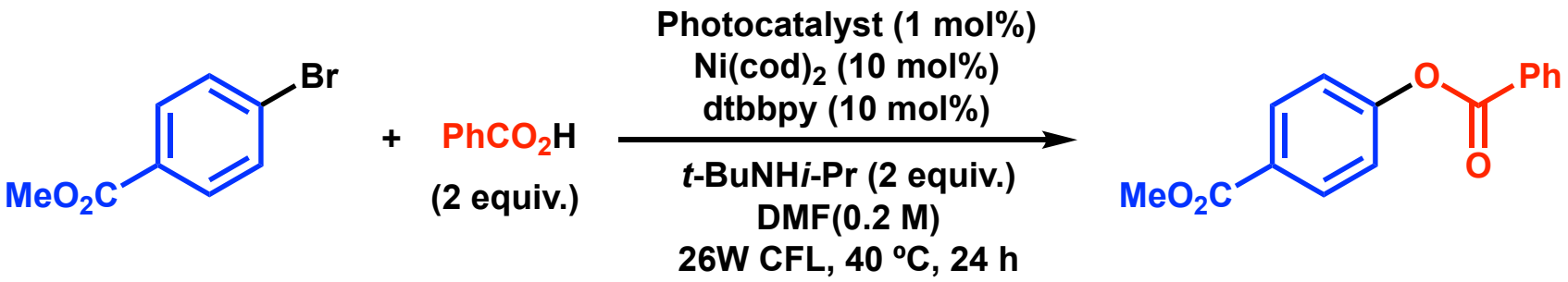

entry	ligand	$E_1/_2$ (Ir^{III*}/Ir^{II}) (V)	yield
1	4,4'-$(CF_3)_2$-bpy	0.74	0
2	4,4'-$(CO_2Me)_2$-bpy	0.70	0
3	bpy	0.61	50
4	4,4'-Me_2-bpy	0.59	65
5	4,4'-$(OMe)_2$-bpy	0.58	70
6	ppy	0.13	85

strong oxidant

oxidizing power

weak oxidant

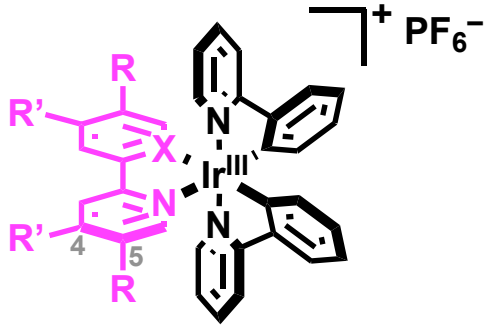

Photocatalyst
= $[Ir^{III}(ppy)_2(ligand)]PF_6$

Ir^{III} = $[Ir^{III}(dF\text{-}CF_3\text{-}ppy)_2(dtbpy)]PF_6$
$E_1/_2$ (Ir^{III*}/Ir^{II}) = 1.21 V

$E_1/_2$ (Ni^{III}/Ni^{II}) = 1.00 V

Welin, E. R., Le. C., Arias, R. D. M., McCusker, J. K., MacMillan, D. W. C. *Science*, **2017**, *355*, 380,

Energy of the Ir-Based Exited State

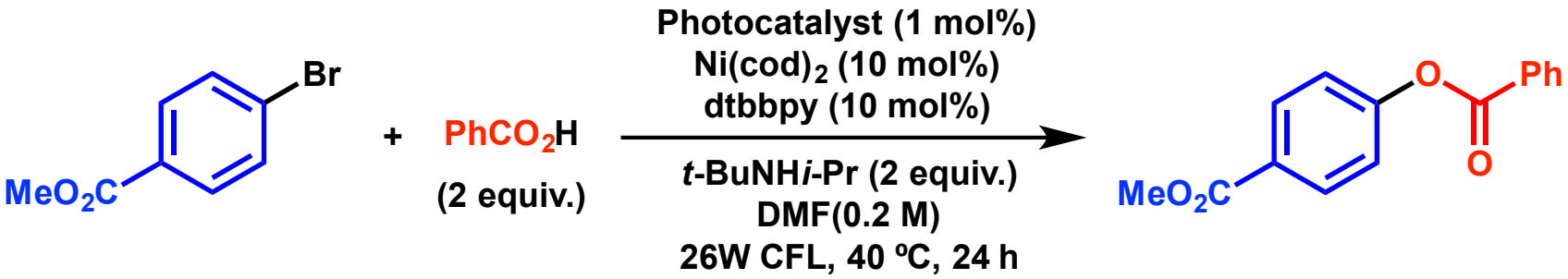

entry	ligand	$E_1/_2$ (Ir^{III*}/Ir^{II}) (V)	E_T(kcal/mol)*	yield
1	4,4'-$(CF_3)_2$-bpy	0.74	39.2	0
2	4,4'-$(CO_2Me)_2$-bpy	0.70	39.7	0
3	bpy	0.61	46.3	50
4	4,4'-Me_2-bpy	0.59	47.6	65
5	4,4'-$(OMe)_2$-bpy	0.58	47.7	70
6	ppy	0.13	53.6	85

Photocatalyst = $[Ir^{III}(ppy)_2(ligand)]PF_6$

* E_T was caluculated from $_{MAX}$ of emission spectrum.

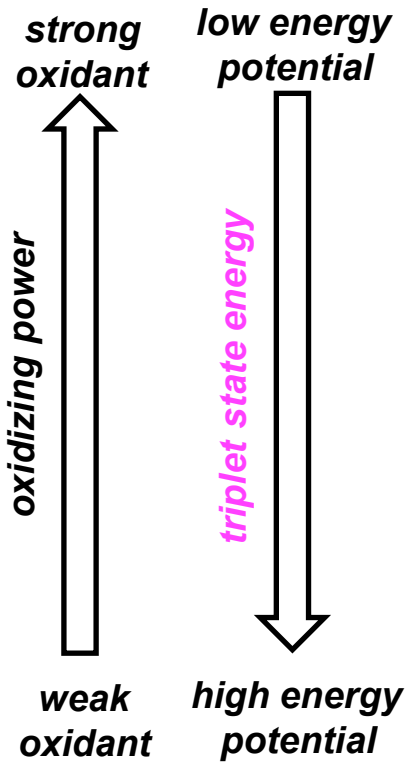

Welin, E. R., Le. C., Arias, R. D. M., McCusker, J. K., MacMillan, D. W. C. *Science*, **2017**, *355*, 380,

Direct Excitation Experiment

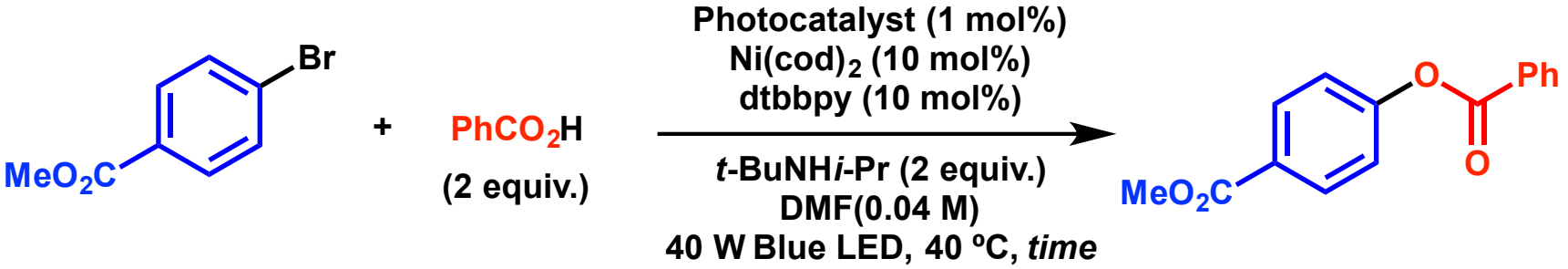

entry	Photocatalyst	*time* (h)	yield
0	$Ir(ppy)_3$	18	85%
1	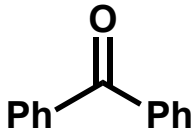	18	25% (brsm: 63%)
2	none	120	45% (brsm: 100%)
3[a]	none	120	0%

[a] Reaction vessel was wrapped in aluminium foil and placed in front of blue LED.

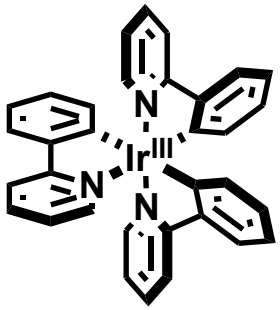

$[Ir^{III}(ppy)_3]$

⇨ coupring reaction would undergo *via* energy transfer pathway

Welin, E. R., Le. C., Arias, R. D. M., McCusker, J. K., MacMillan, D. W. C. *Science*, **2017**, *355*, 380,

Stoichiometric Studies with Arylnickel(II) Complex

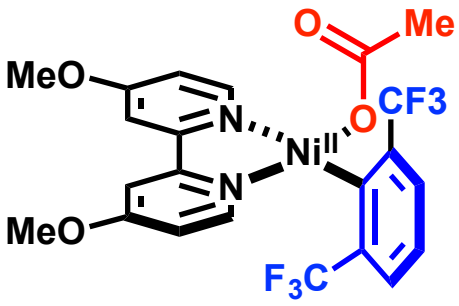

Photocatalyst (0.625 mol%)

t-BuNH*i*-Pr (2 equiv.)
DMF-d^7(0.01 M)
40 W Blue LED, 40 °C, *time*

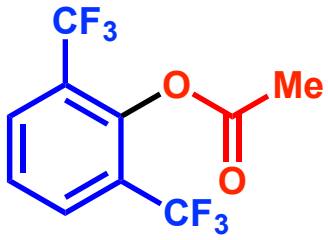

entry	Photocatalyst	*time* (h)	ArOCOMe[a]
1	Ir(ppy)$_3$	30 min	detected
2	none	60 h	detected
3[b]	none	60 h	not detected

[a] Reaction was accessed by ^{19}F NMR.
[b] Reaction vessel was wrapped in aluminium foil and placed in front of blue LED.

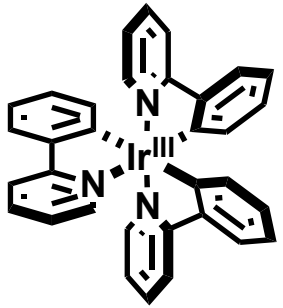

[Ir^{III}(ppy)$_3$]

Proposed Catalytic Cycle

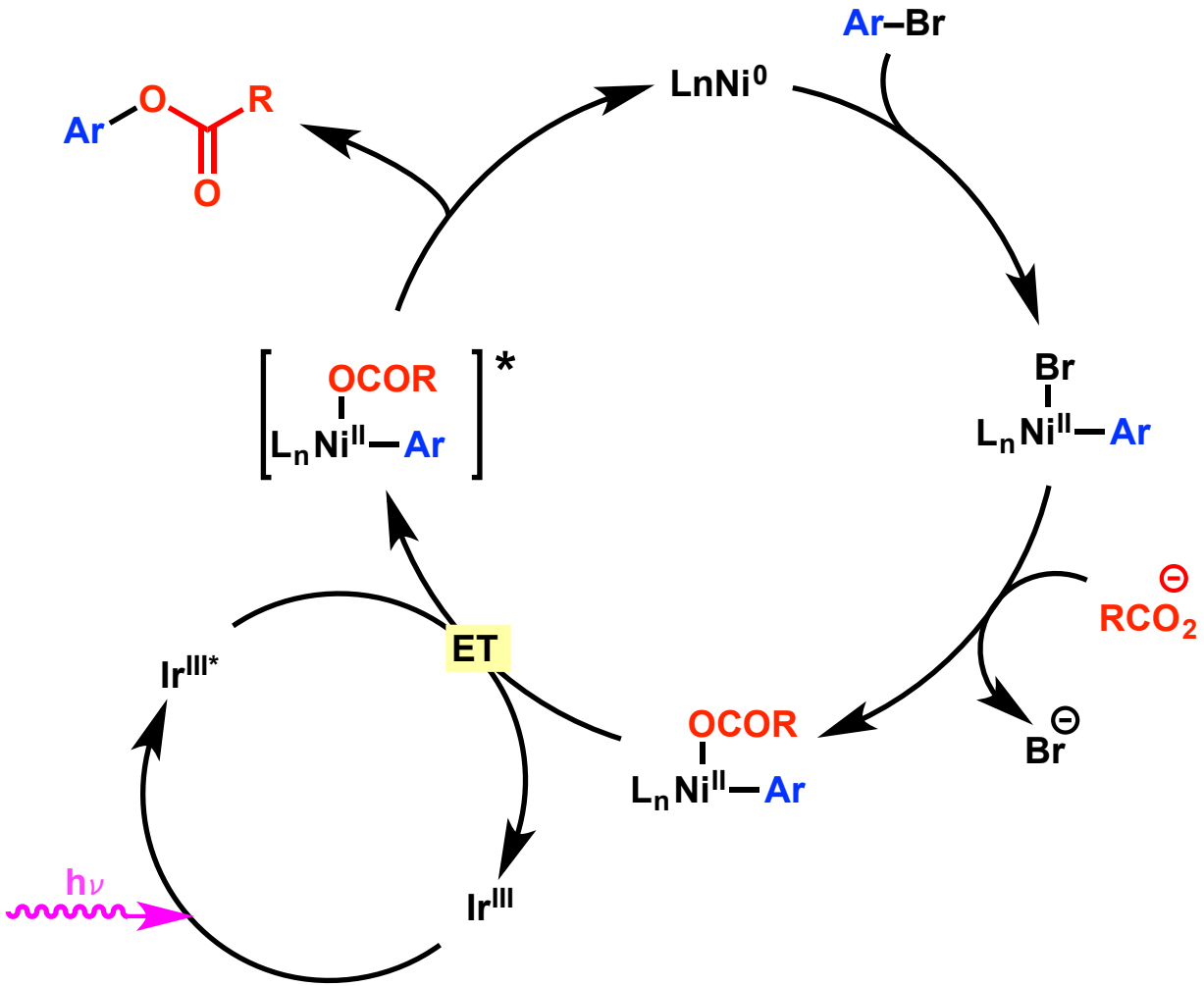

Welin, E. R., Le. C., Arias, R. D. M., McCusker, J. K., MacMillan, D. W. C. *Science*, **2017**, *355*, 380,

Substrate Scope of Carboxylic Acid

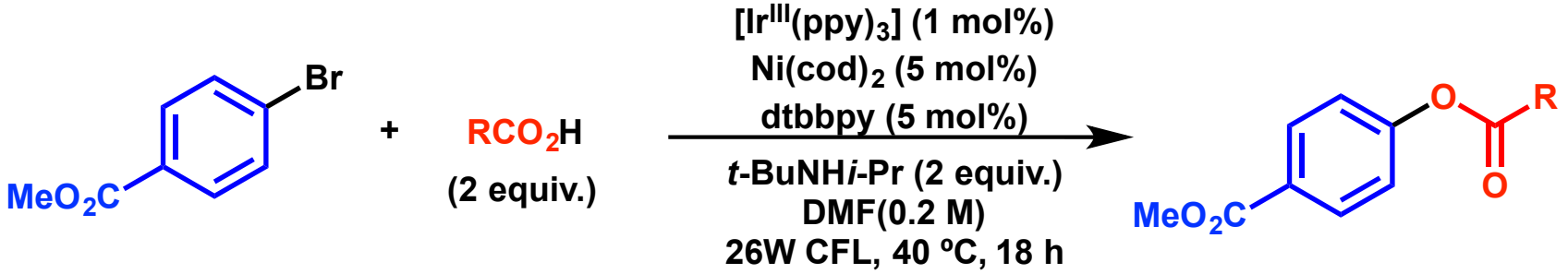

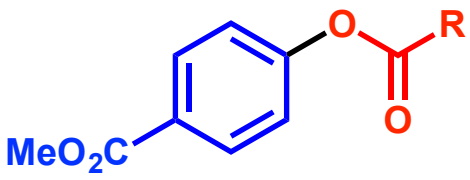

R = Me:76%
R = *c*-hex: 81%
R = *t*-Bu: 79%
R = Ad: 80%

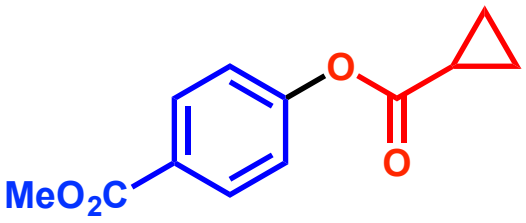

83%

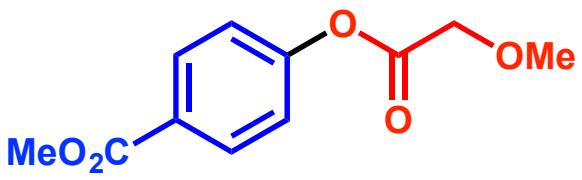

76%

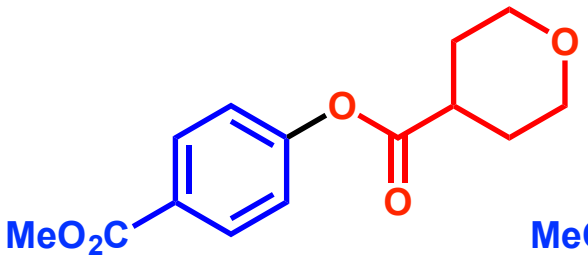

80%

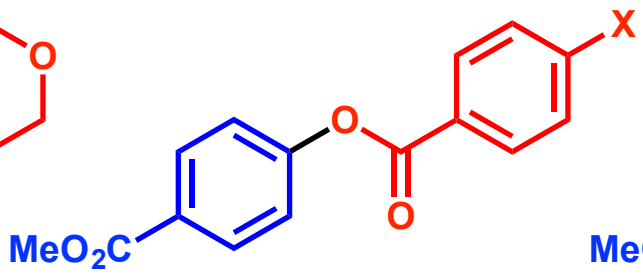

X = F: 93%
X = OMe: 95%

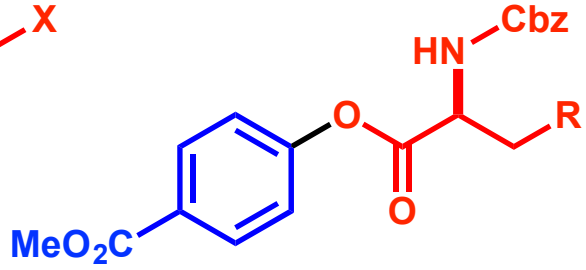

R = Ph: 86%
R = *i*-Pr: 81%

Welin, E. R., Le. C., Arias, R. D. M., McCusker, J. K., MacMillan, D. W. C. *Science*, **2017**, *355*, 380,

Substrate Scope of Aryl Bromide

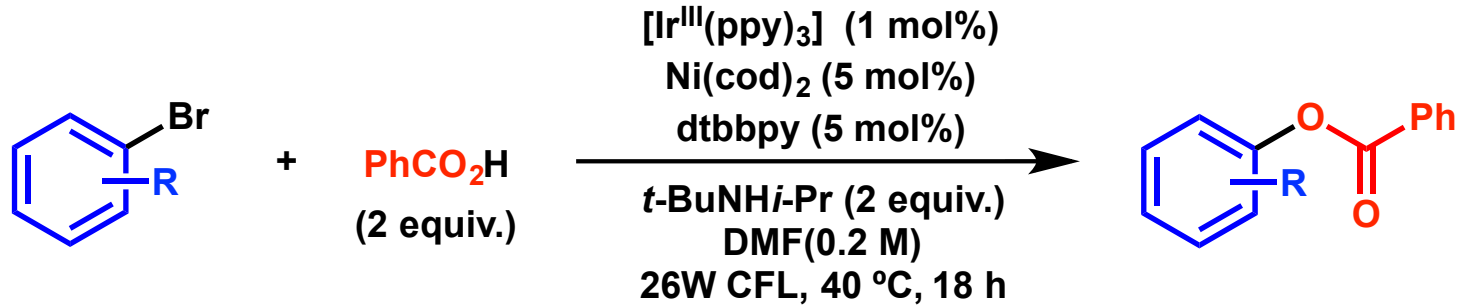

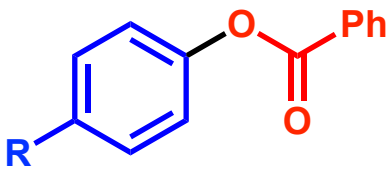

R = Ac: 86%
R = CF_3: 86%

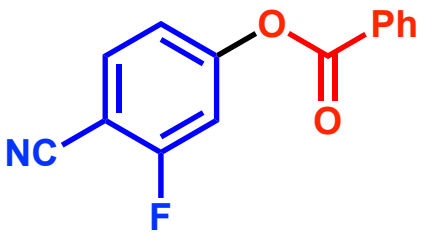

R = 81%

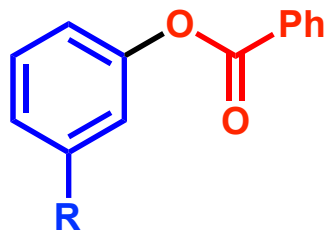

R = Cl: 68%
R = CF_3: 86%

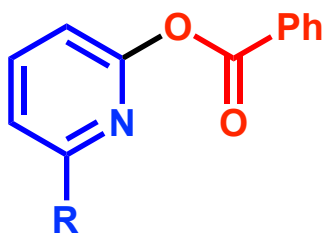

R = Me: 95%
R = CF_3: 87%

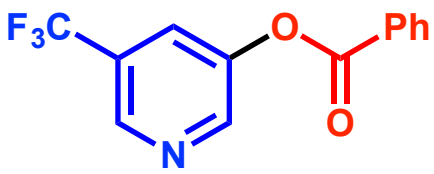

62%

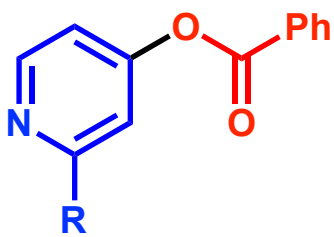

R = Me: 84%
R = CF_3: 86%

Welin, E. R., Le. C., Arias, R. D. M., McCusker, J. K., MacMillan, D. W. C. *Science*, **2017**, *355*, 380,

Possible Energy Transfer Mechanism

① **Förster resonance energy transfer**

nonradiative dipole–dipole coupling

- **efficiency is depends on the overlap integral of the donor emission spectrum with the acceptor absorption**
- **distance between D and A: 10~100 Å**

② **Dexter energy transfer**

electron exchange between A and D

- **efficiency is depends on the wavefunction overlap between the donor and acceptor**
- **distance between D and A: <10Å**

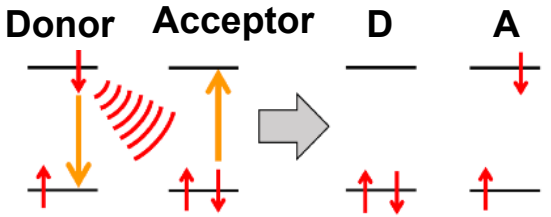

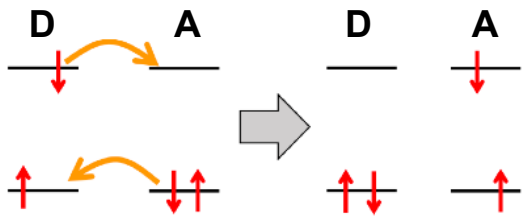

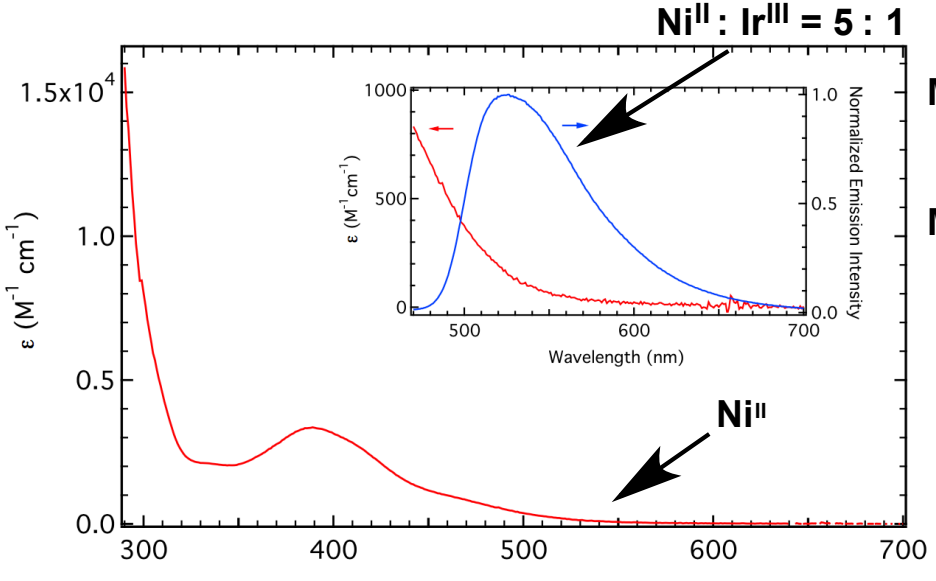

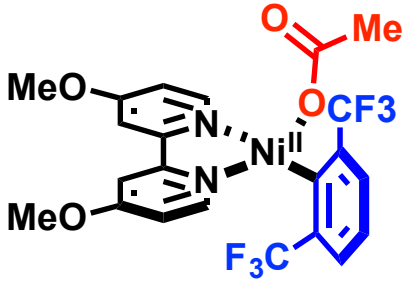

Ni^{II}

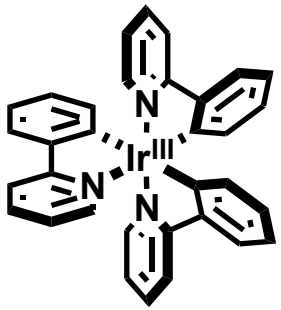

Ir^{III}

Figure 3. Electronic Absorption Spectrum. Main graph: Electronic absorption spectrum of Ni^{II}. Inset: Overlap between the emission of Ir^{III}* and the absorbance of Ni^{II}.

small degree of overlap

Dexter transfer is likely playing an important role in the reductive elimination step

Welin, E. R., Le. C., Arias, R. D. M., McCusker, J. K., MacMillan, D. W. C. *Science*, **2017**, *355*, 380,

Detailed Excitation Mechanism

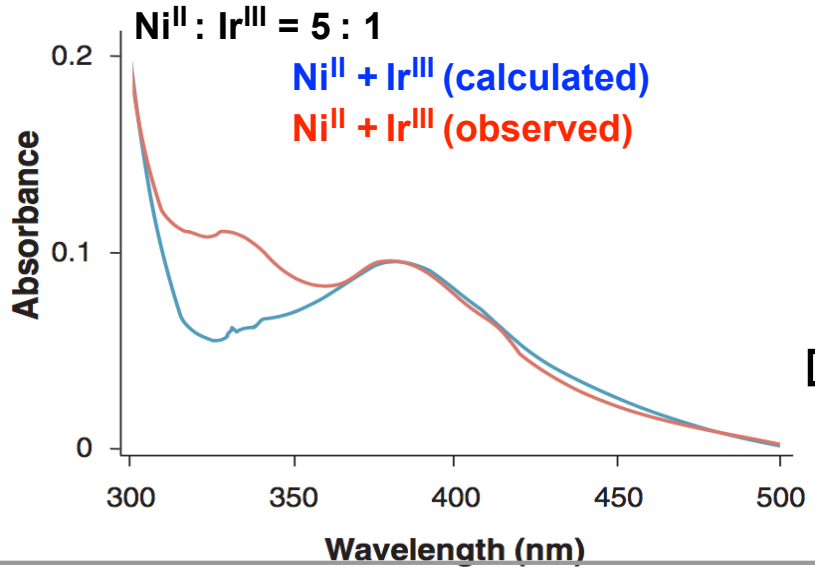

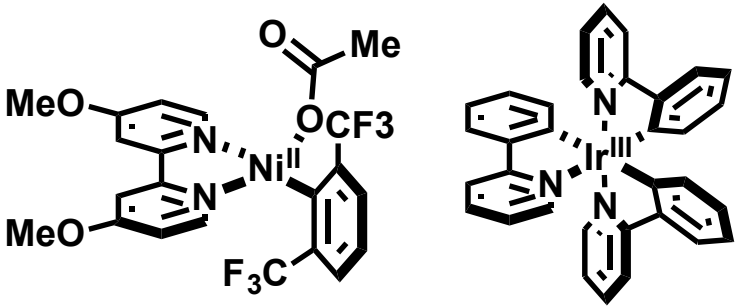

association between Ni^{II} and Ir^{III} was suggested

œÄ–œÄ interaction between dmbpy and ppy?

Figure 4. UV-Vis spectrum of Ni^{II} and Ir^{III}

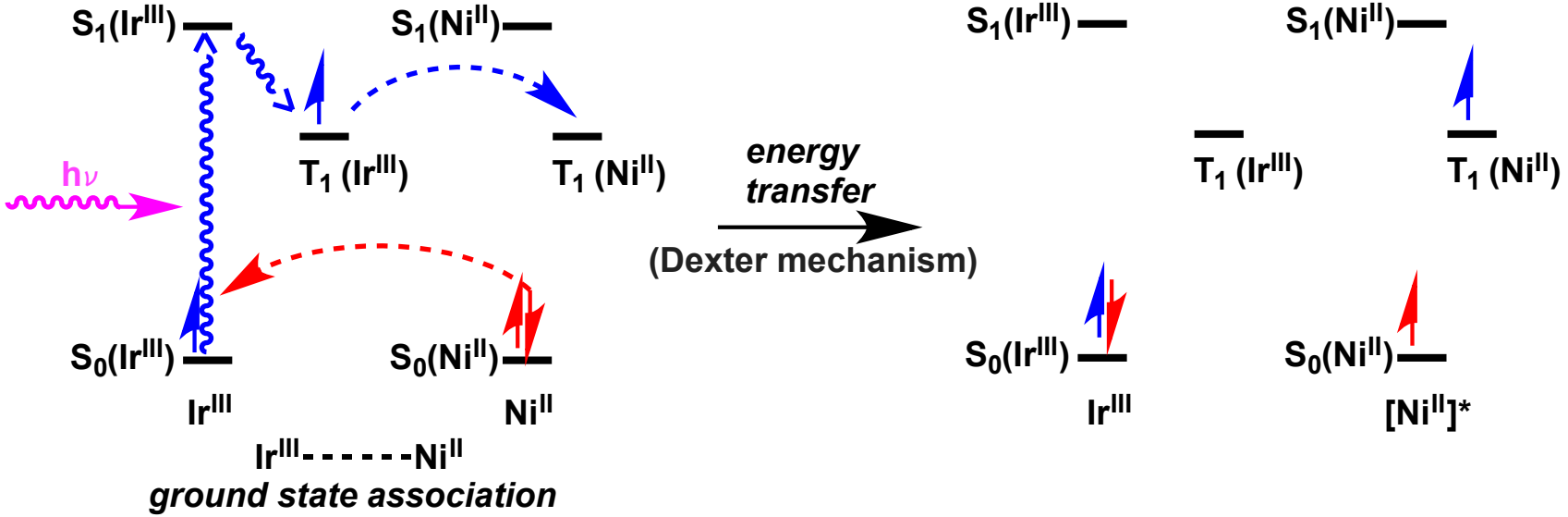

Proposed Mechanism for R. E. (My proposal)

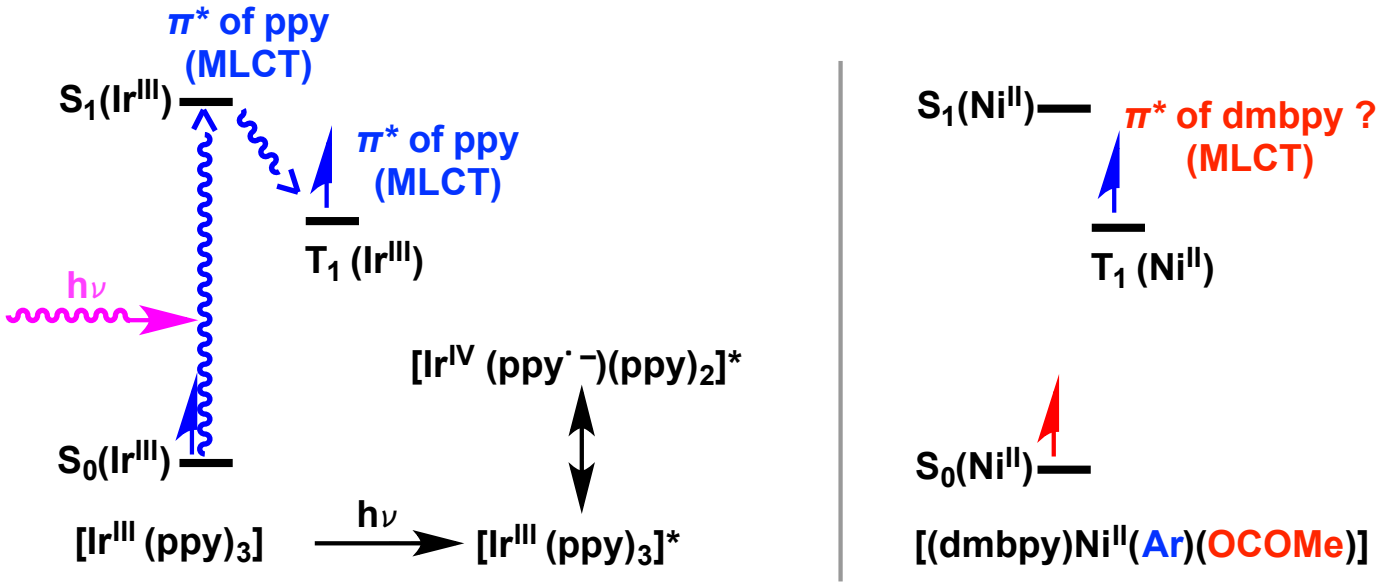

It is well known that transition $S_0(Ir^{III})$ to $S_1(Ir^{III})$ and $T_1(Ir^{III})$ is metal to ligand charge transfer (MLCT)

If transition S_0 (Ni^{II}) to T_1 (Ni^{II}) is MLCT (Ni^{II} to dmbpy), electron deficient Ni^{III+} would undergo reductive relimination

[(dmbpy)Ni^{II}(Ar)(OCOMe)]* ⟷ [(dmbpy$^{\cdot -}$)Ni^{III}(Ar)(OCOMe)]*

↓ –[(dmbpy$^{\cdot -}$)Ni^{I}]*

ArOCOMe

dmbpy = 4,4-dimethoxybipyridine

Summary

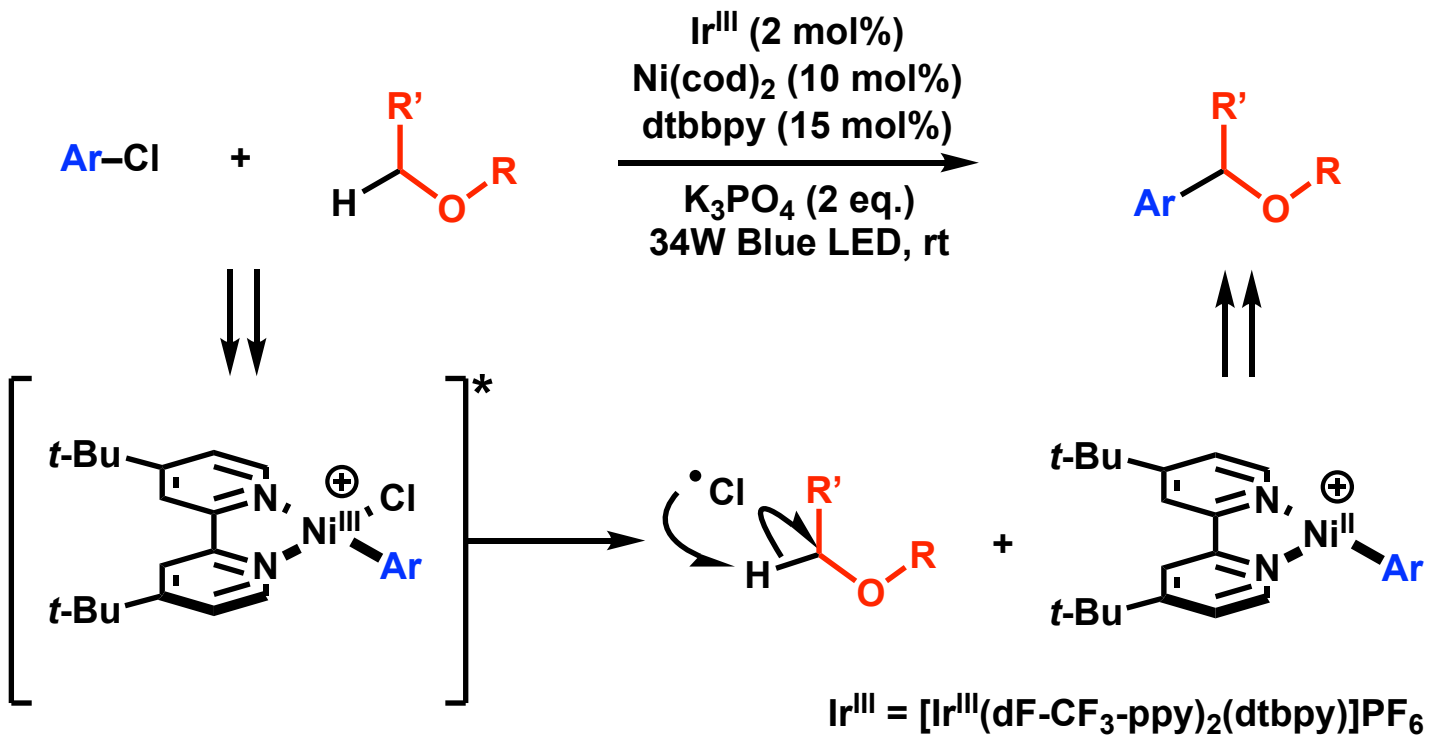

Shieds, B. J., Doyle, A. G. *J. Am. Chem. Soc.* **2016**, *138*, 12722

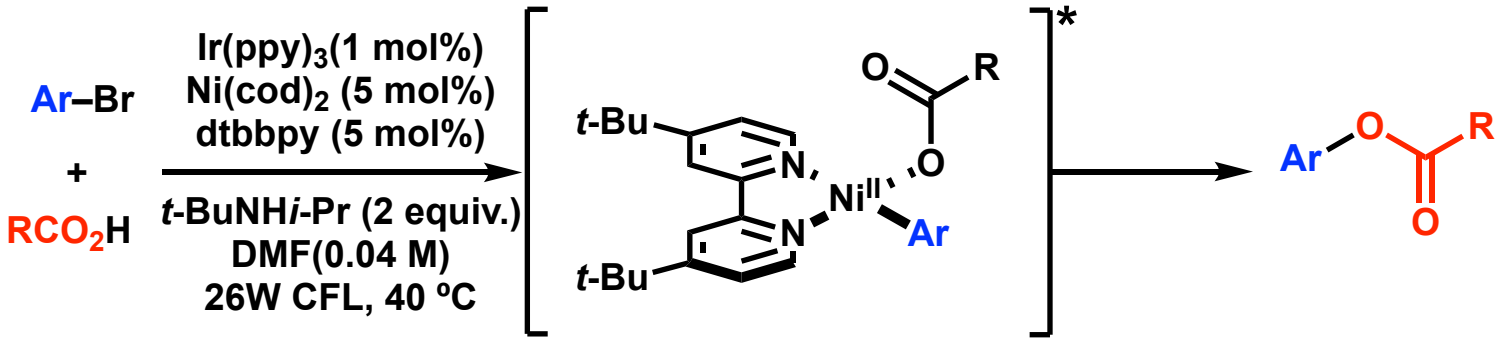

Welin, E. R., Le. C., Arias, R. D. M., McCusker, J. K., MacMillan, D. W. C. *Science*, **2017**, *355*, 380,

Appendix

Absorbance of $[Ni^{III}Cl_3]^+$ Complex

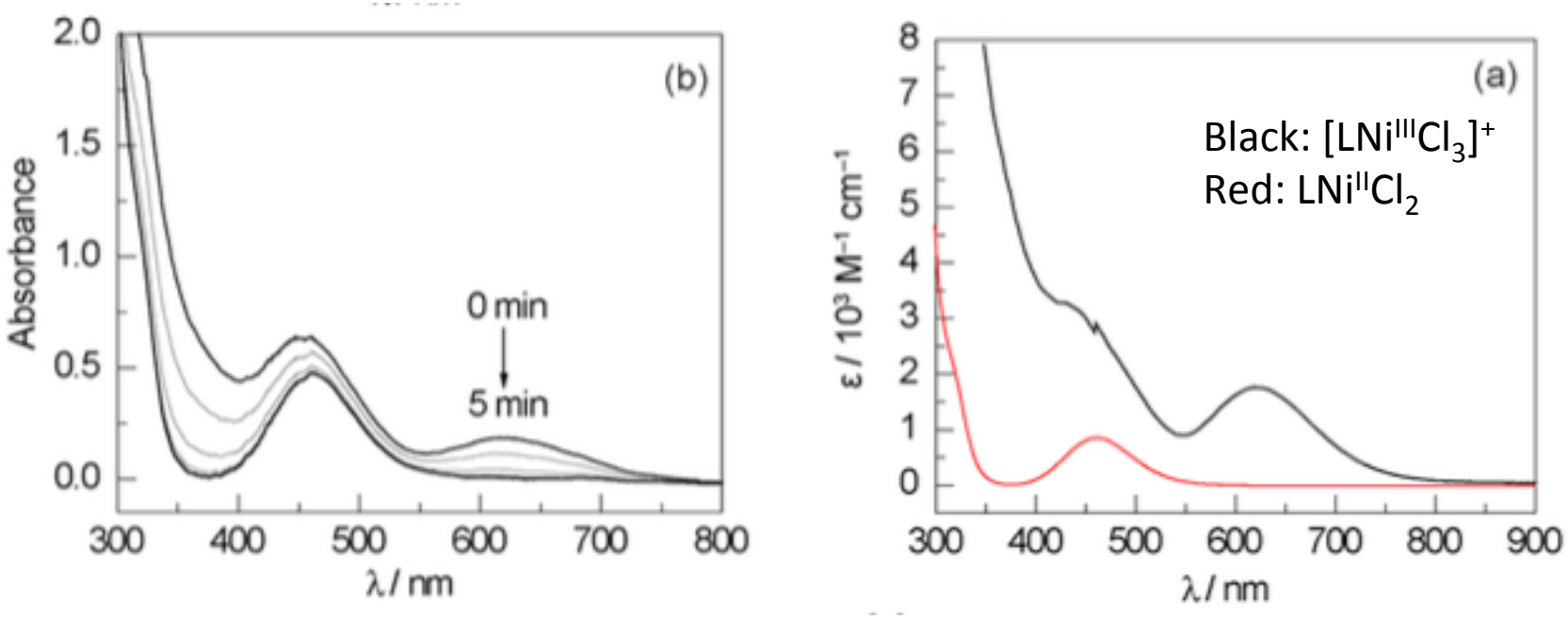

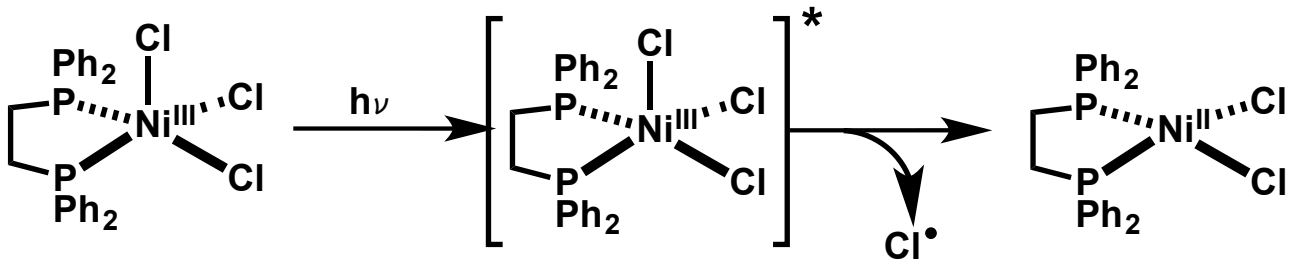

Hwang, S. J., Powers, D. C. Maher, A. G., Anderson, B. L., Hadt, R. G., Zheng, S-L., Chen, Y-S., Nocera, D. G. *J. Am. Chem. Soc*, **2015**, *137*, 6472

Halogene Exchange Experiment

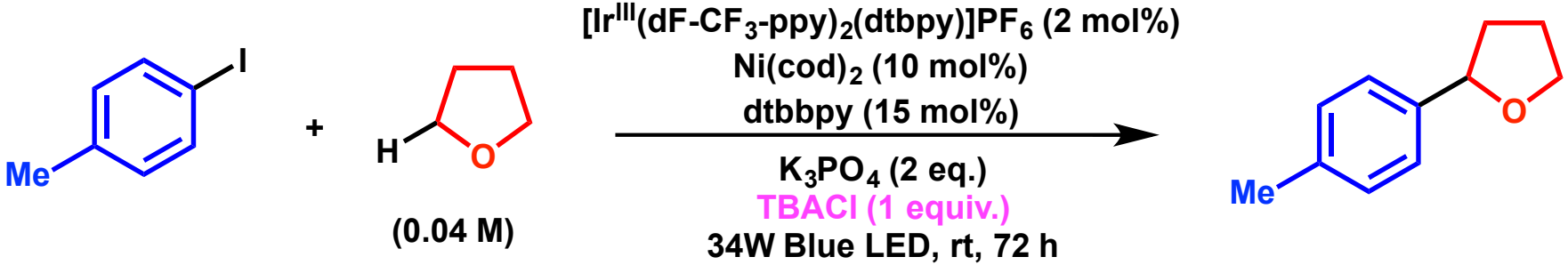

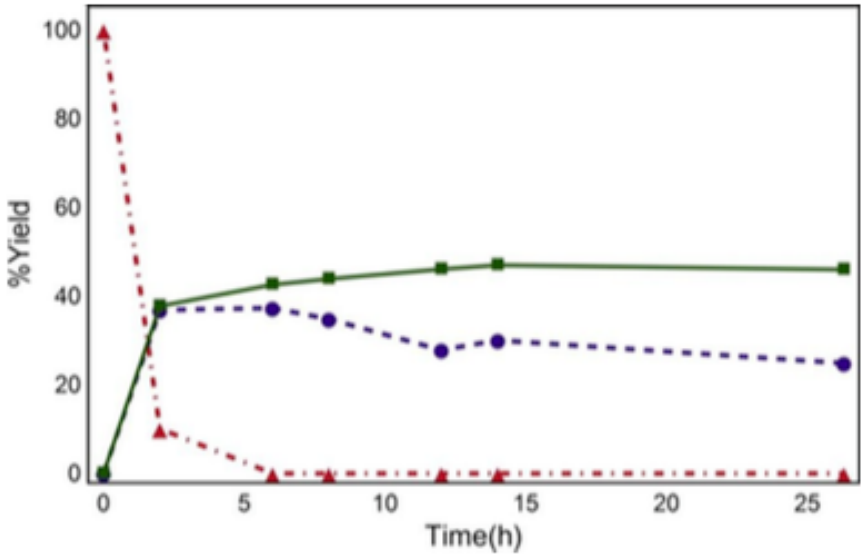

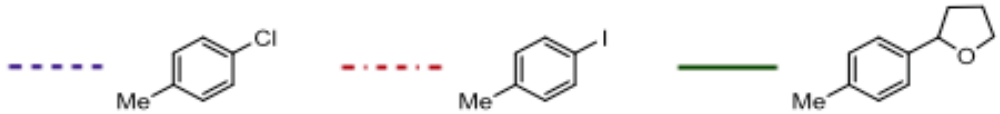

Shieds, B. J., Doyle, A. G. *J. Am. Chem. Soc.* **2016**, *13*8, 12722

Lamp Emission Data (Doyle's Work)

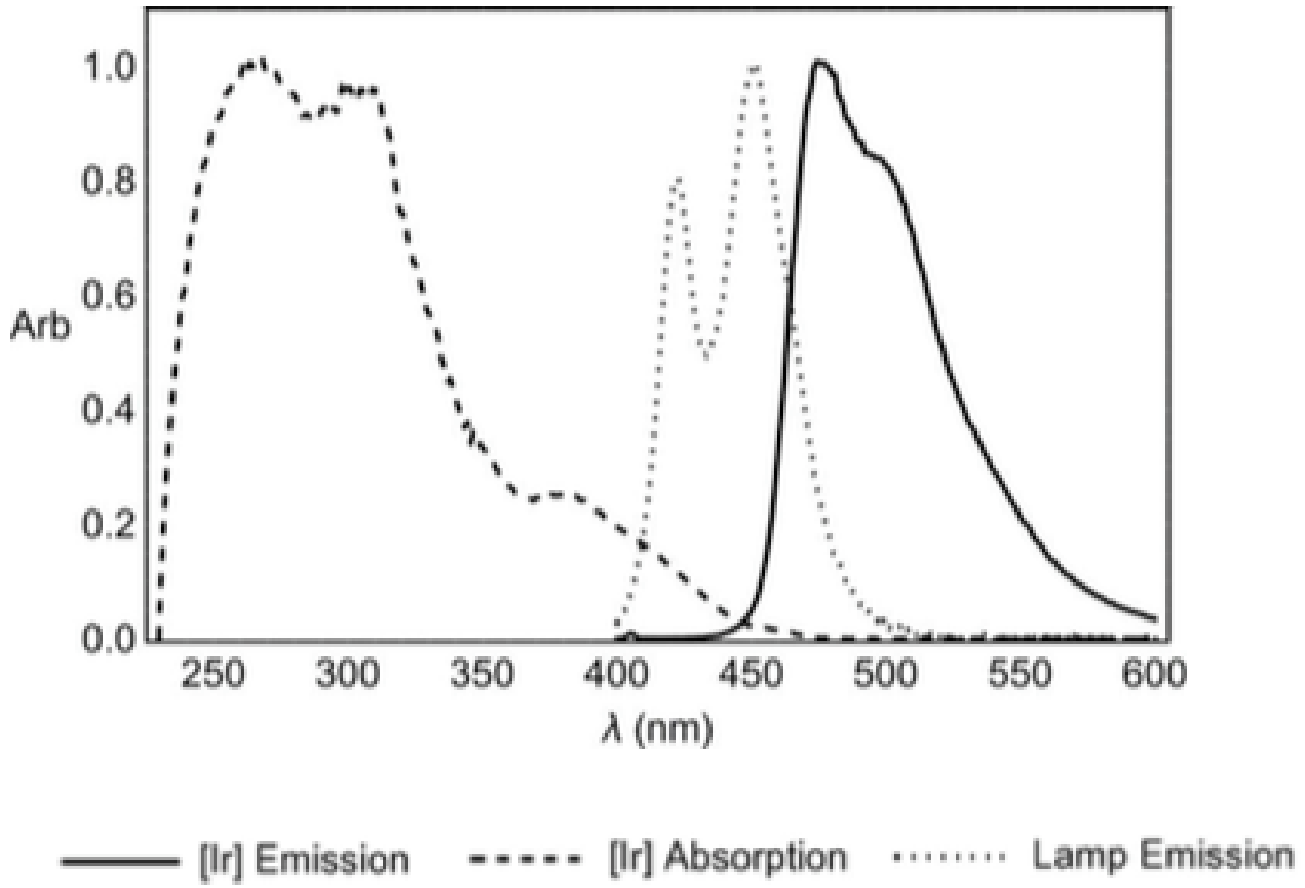

Shieds, B. J., Doyle, A. G. *J. Am. Chem. Soc.* **2016**, *13*8, 12722

Absorbance of [(tbbpy)Ni^{II}(tol)Cl]

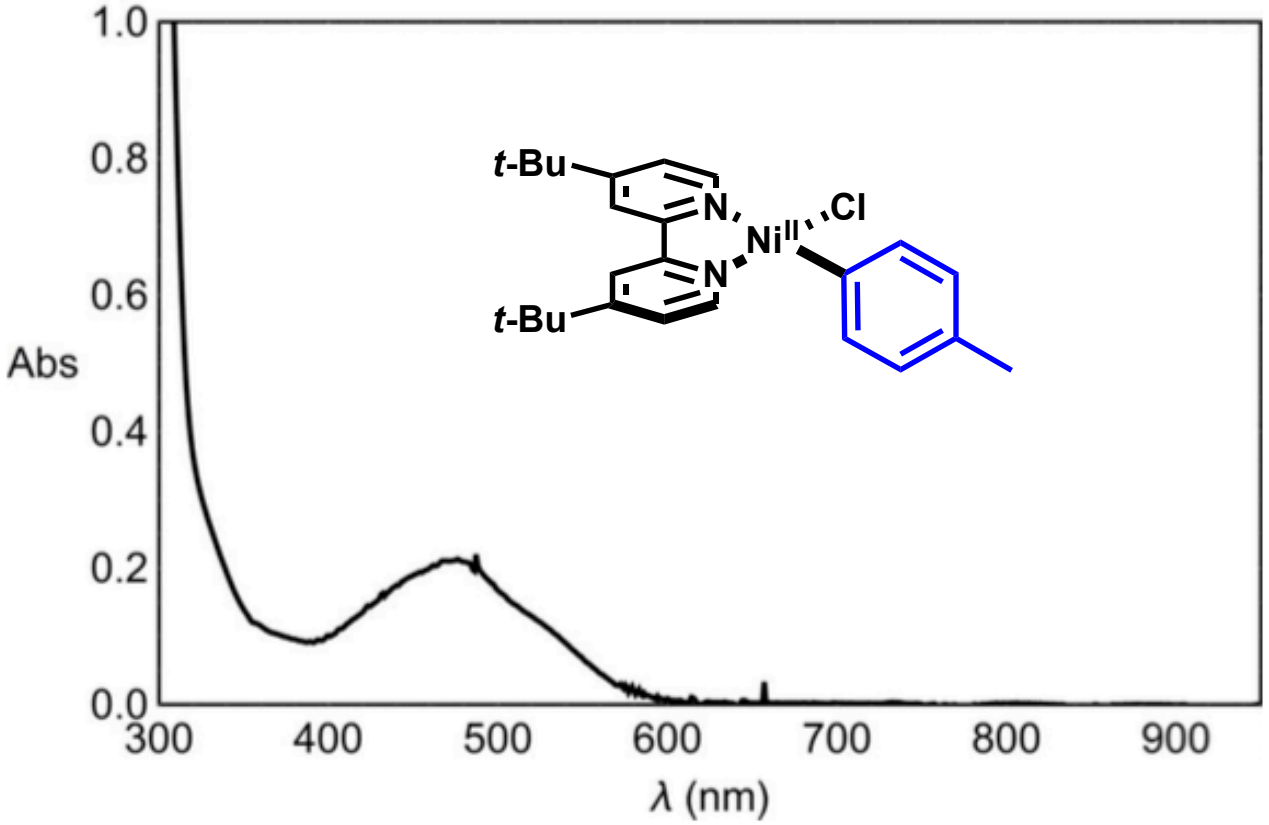

Shieds, B. J., Doyle, A. G. *J. Am. Chem. Soc.* **2016**, *13*8, 12722

Stoichiometric Oxidation Using Ir^{III} as an Oxidant

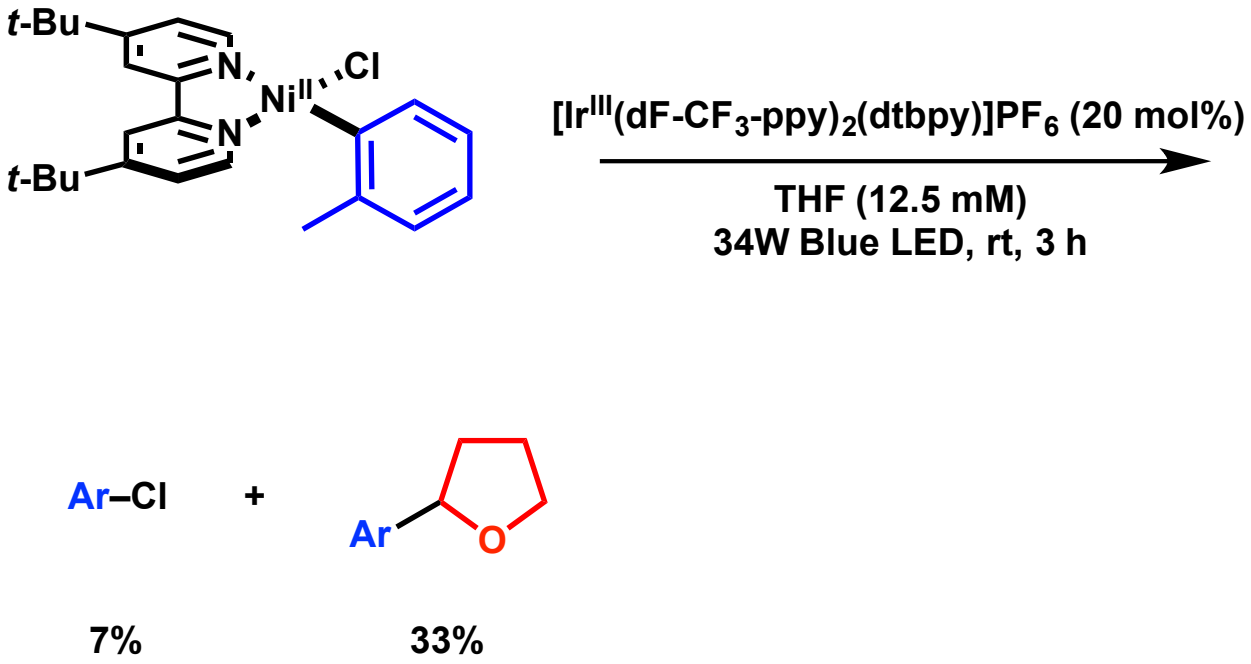

Cyclic Voltammetry Data

Cyclic Voltammetry was performed on a CH Instruments Electrochemical Analyzer (CH1600E). A 1 mM solution of (dtbbpy)Ni(*o*-tolyl)Cl with 0.1 M tetrabutylammonium hexafluorophosphate as a supporting electrolyte in THF was prepared in a nitrogen filled glove box. The solution was removed from the glove box and a cyclic voltammogram was obtained under nitrogen atmosphere using a glassy carbon working electrode, a platinum mesh counter electrode, and a saturated calomel reference electrode. Scan rate = 0.01 Vs^{-1}.

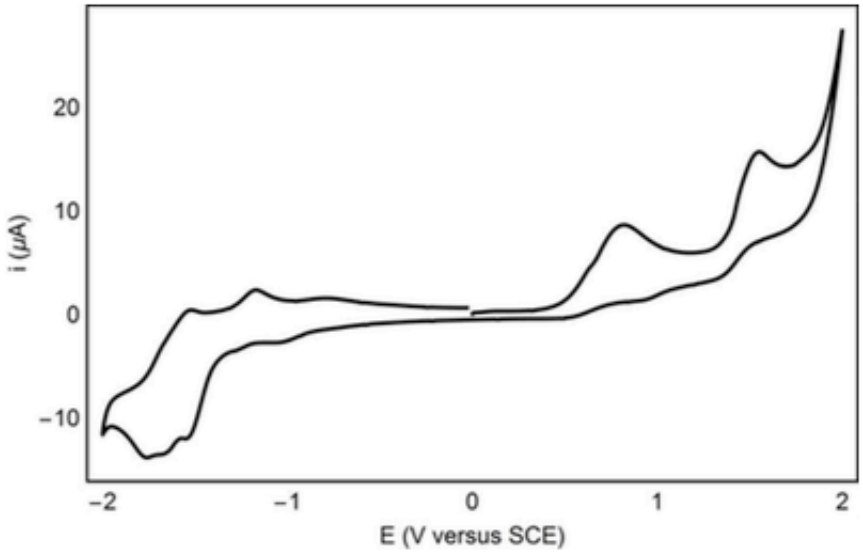

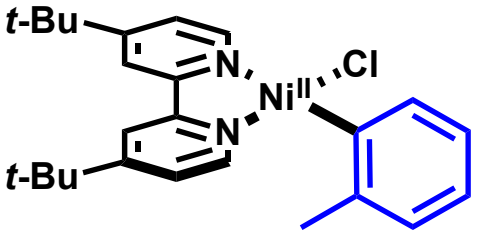

Fig. S32. Cyclic voltammogram of (dtbbpy)Ni(*o*-tolyl)Cl shows an irreversible first oxidation at E_p = 0.85 V versus SCE in THF which corresponds to the Ni^{II}/Ni^{III} redox couple and an irreversible first reduction at E_p = – 1.17 V versus SCE in THF which corresponds to the Ni^{I}/Ni^{II} redox couple. Remaining peaks could not be assigned due to the irreversible nature of the first oxidation and reduction.

Shieds, B. J., Doyle, A. G. *J. Am. Chem. Soc.* **2016**, *13*8, 12722

Calculated Relevant Molecular Orbitals

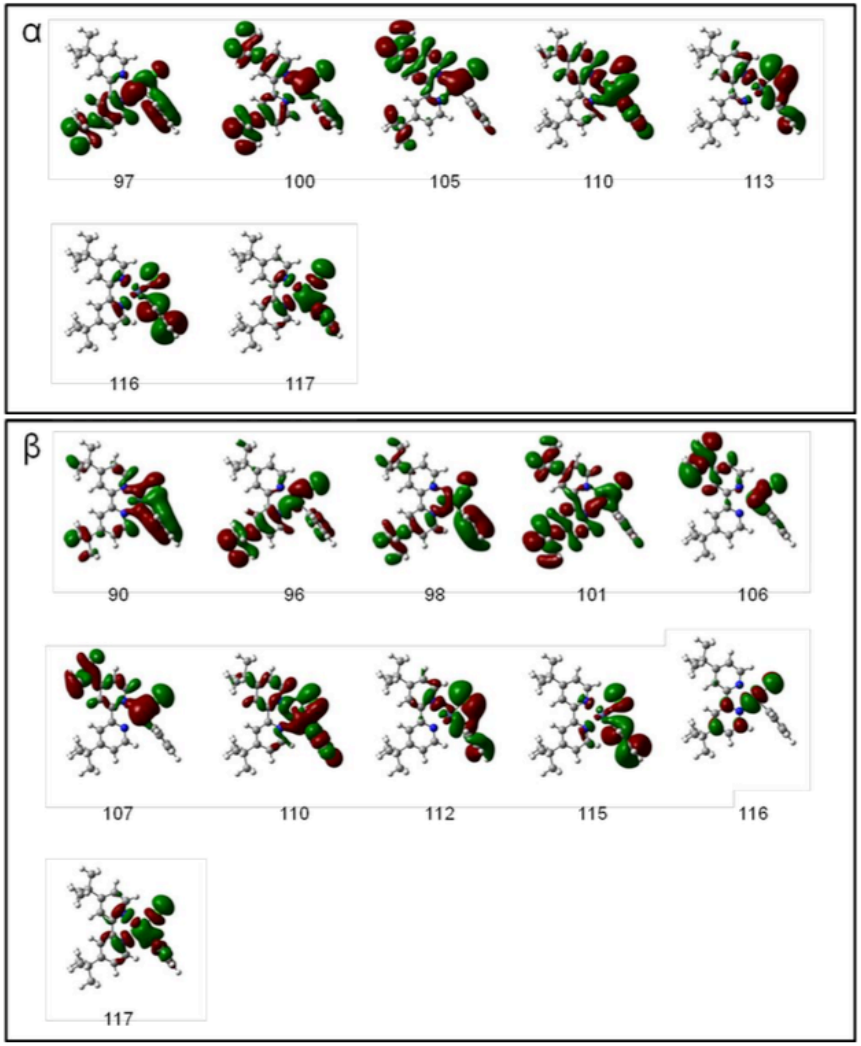

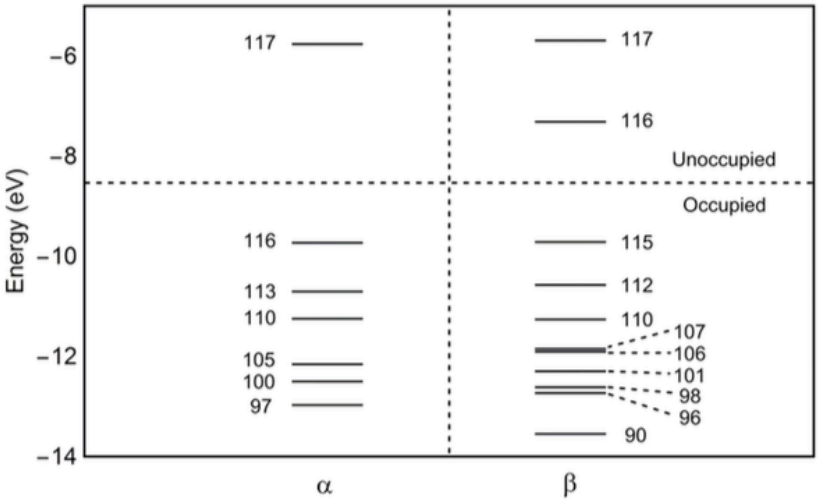

Calculations were performed on Gaussian 09 D.01 software suite *(37)*. For all calculations the B3LYP hybrid exchange-correlation functional was used. Gas-phase geometry optimization and frequency calculations were carried out using a SDD basis set for Ni and Cl and 6-31G* for all other atoms. Optimization and frequency calculations for thermochemistry were carried out using a SDD basis for Ni and Cl and 6-311++G for all other atoms with the SMD (THF) solvation model. All frequency calculations gave no imaginary frequencies. Time-dependent DFT (TD-DFT) calculations were carried out on the gas-phase optimized geometry using the TZVP basis set.**

DFT-Calculated Transitions

Excited State	λ (nm)	Energy (kcal mol^{-1})	f	Contributions
1	689	46	0.0076	116α → 117α (74%) 115β → 117β (12%)
2	486	65	0.0049	113α → 117α (11%) 109β → 116β (28%) 111β → 116β (26%) 115β → 117β (15%)
3	460	68	0.0092	109β → 116β (10%) 111β → 116β (17%) 112β → 117β (26%) 115β → 117β (18%)
4	401	78	0.0075	110α → 117α (29%) 107β → 117β (22%) 110β → 117β (13%) 115β → 117β (10%)
5	396	79	0.0025	114α → 118α (40%) 113β → 118β (38%)
6	392	80	0.0209	113α → 117α (33%) 112β → 117β (12%)
7	375	84	0.022	106β → 117β (11%) 107β → 117β (19%) 115β → 117β (31%)

Table S15. TD-DFT calculated transitions for $[Ni(dtbbpy)(Ph)Cl]^+$ (**5a**). Transitions f > 0.0025 are shown. Orbital contributions ≥ 10% are shown of which Ni–Cl σ → σ* transitions are in red.

Optimization of Reaction Conditions

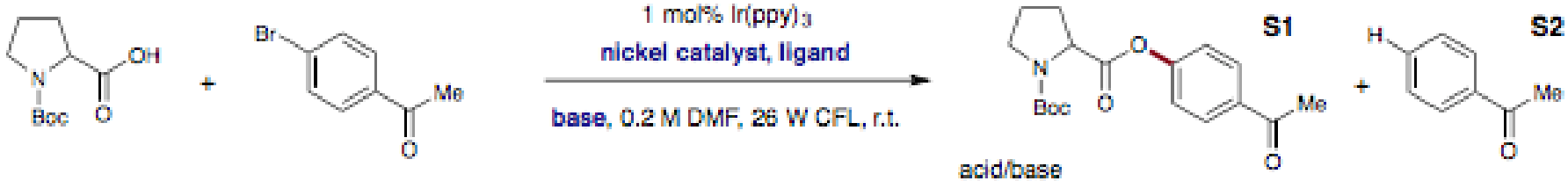

entry	base	no. of lamps	nickel catalyst	ligand	acid/base equiv.	Ni/L mol%	yield **S1**	yield **S2**
1	Cs_2CO_3	1	$NiCl_2$•DME	dtbbpy	3	10 mol%	49%	30%
2	DBU	1	$NiCl_2$•DME	dtbbpy	3	10 mol%	59%	8%
3	DBU	2	$NiCl_2$•DME	dtbbpy	3	10 mol%	62%	13%
4	DBU	2	$NiBr_2$•diglyme	dtbbpy	3	10 mol%	70%	12%
5	DBU	2 + fan	$NiBr_2$•diglyme	dtbbpy	3	10 mol%	69%	12%
6	DBU	2	$NiBr_2$•diglyme	bpy	3	10 mol%	62%	13%
7	DBU	2	$NiBr_2$•diglyme	4,4'-dOMebpy	3	10 mol%	68%	13%
8	DBU	2	$NiBr_2$•diglyme	4,4'-dMebpy	3	10 mol%	56%	9%
9	NEt_3	2	$NiBr_2$•diglyme	dtbbpy	3	10 mol%	43%	14%
10	*i*-Pr_2NEt	2	$NiBr_2$•diglyme	dtbbpy	3	10 mol%	41%	23%
11	*i*-Pr_2NH	2	$NiBr_2$•diglyme	dtbbpy	3	10 mol%	74%	12%
12	*n*-Bu_2NH	2	$NiBr_2$•diglyme	dtbbpy	3	10 mol%	67%	17%
13	*t*-BuNH*i*-Pr	2	$NiBr_2$•diglyme	dtbbpy	3	10 mol%	84%	9%
14	*t*-BuNH*i*-Pr	2	$NiBr_2$•diglyme	dtbbpy	2	10 mol%	84%	11%
15	*t*-BuNH*i*-Pr	2	$NiBr_2$•diglyme	dtbbpy	1	10 mol%	40%	10%
16	***t*-BuNH*i*-Pr**	**2**	**$NiBr_2$•diglyme**	**dtbbpy**	**2**	**5 mol%**	**85%**	**9%**
17	*t*-BuNH*i*-Pr	2	$NiBr_2$•diglyme	dtbbpy	2	2 mol%	67%	9%

Welin, E. R., Le. C., Arias, R. D. M., McCusker, J. K., MacMillan, D. W. C. *Science*, **2017**, *355*, 380,

Emission Spectrum of Ir^{III} Complexes

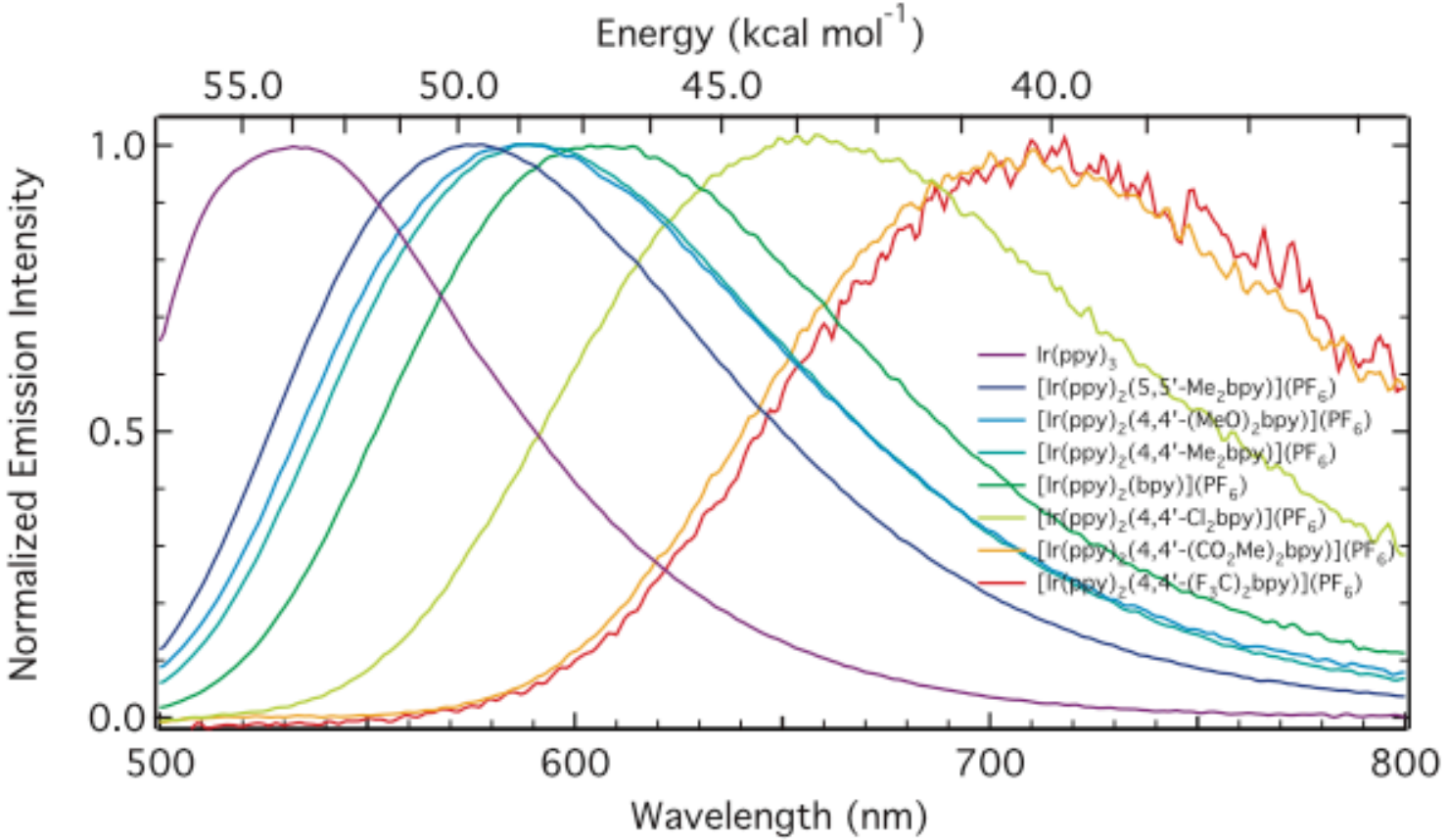

Figure S9. Emission spectra were converted from wavelength to energy units (*59*). E(^{3}MLCT) were calculated by a single mode fit of the steady-state emission spectrum, as described by Claude and Meyer (*60*). Excited state oxidation potentials ($E_{1/2}^{II/III*}$) were calculated as described in reference 14.

Cyclic Voltammetry Data

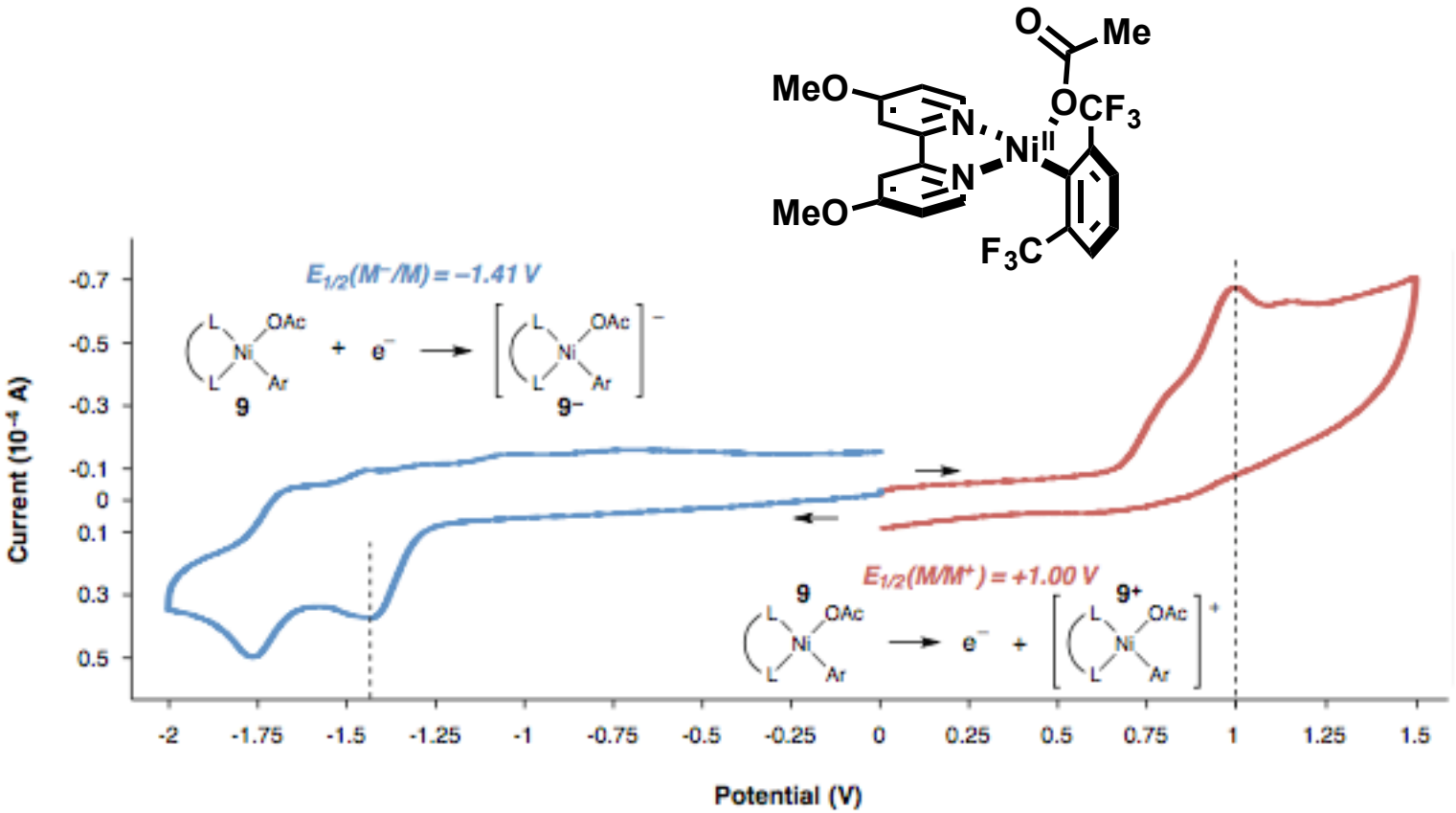

Figure S11. Cyclic voltammetry suggests against a redox-induced mechanism. Voltammogram measured in DMF against SCE at 0.01 M of **9** with 0.2 M NH_4PF_6 as supporting electrolyte with a scan rate of 5 V/s.

Welin, E. R., Le. C., Arias, R. D. M., McCusker, J. K., MacMillan, D. W. C. *Science*, **2017**, *355*, 380,

Quenching Experiments

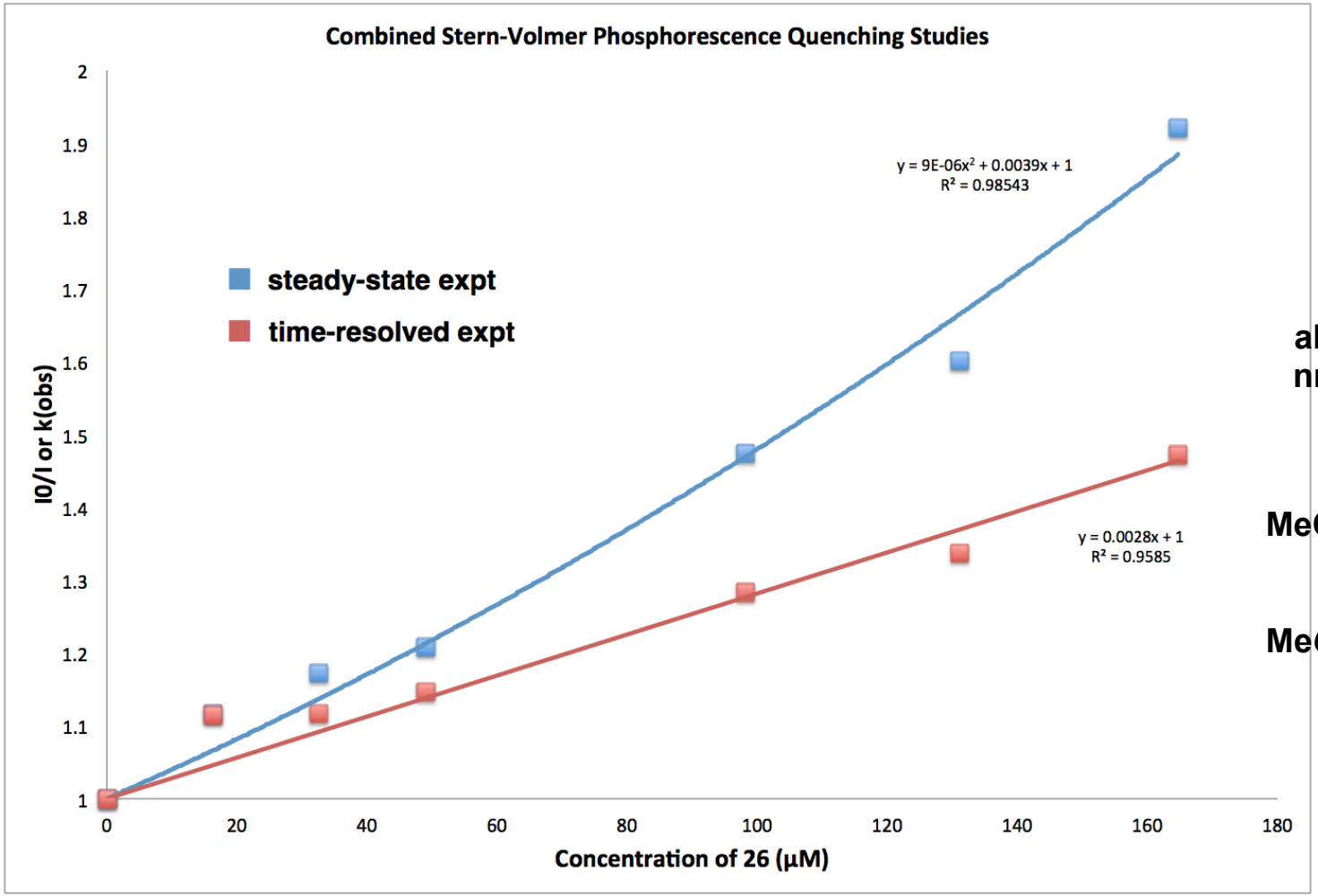

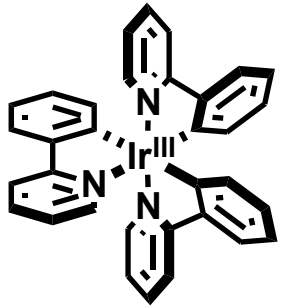

absorbance at 400 nm was used

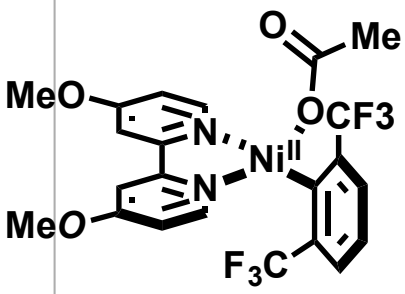

(quencher)

$$I_0/I = 1 + k_q t_0[Q]$$

Welin, E. R., Le. C., Arias, R. D. M., McCusker, J. K., MacMillan, D. W. C. *Science*, **2017**, *355*, 380,

Quenching Experiments

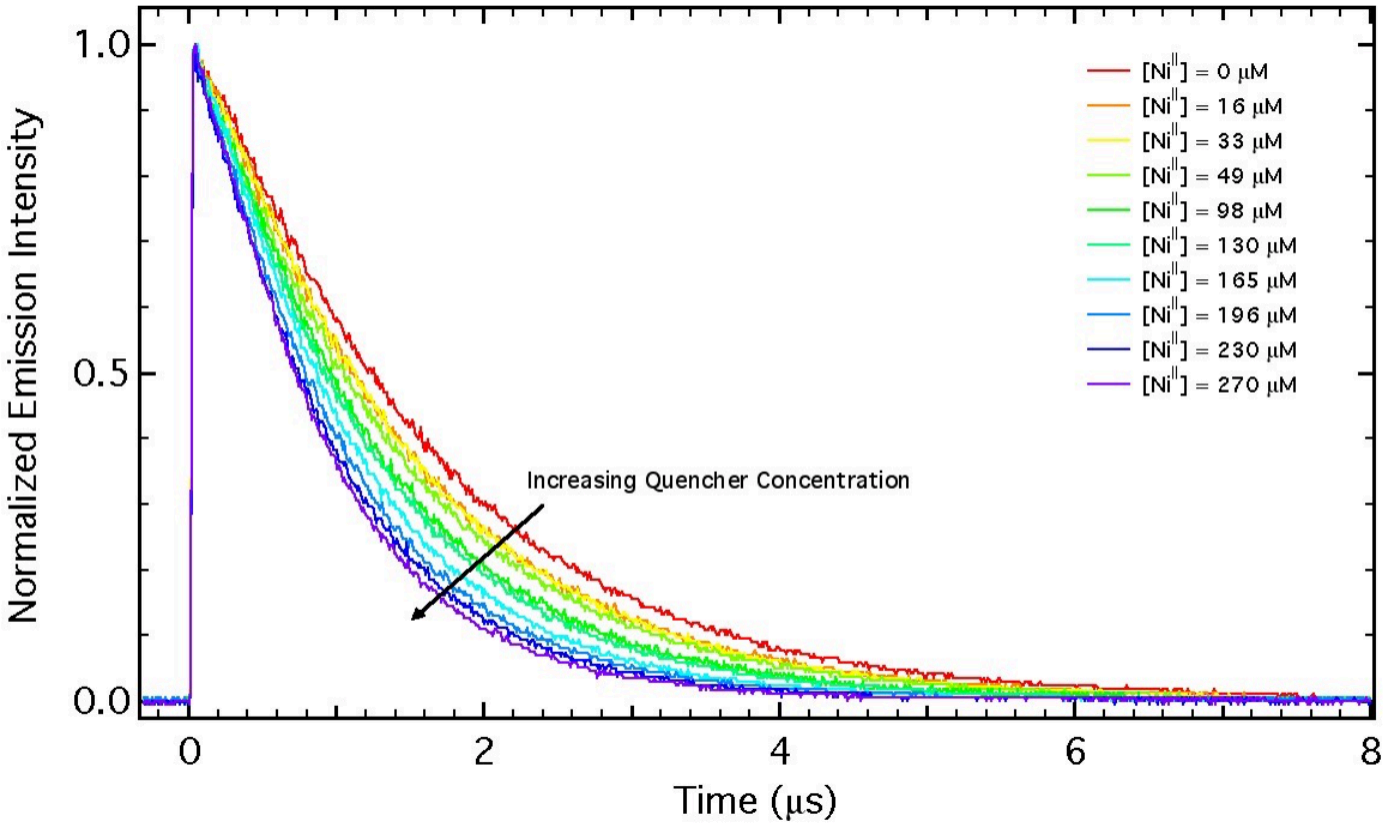

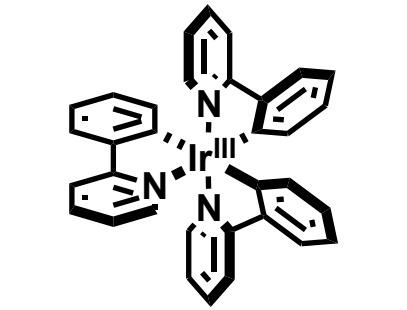

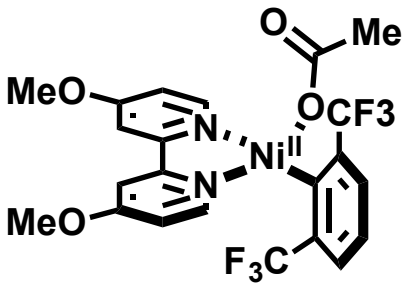

(quencher)

Figure S19. Time-Resolved Stern-Volmer Experiment.

Excitation of $Ir^{III}(ppy)_3$

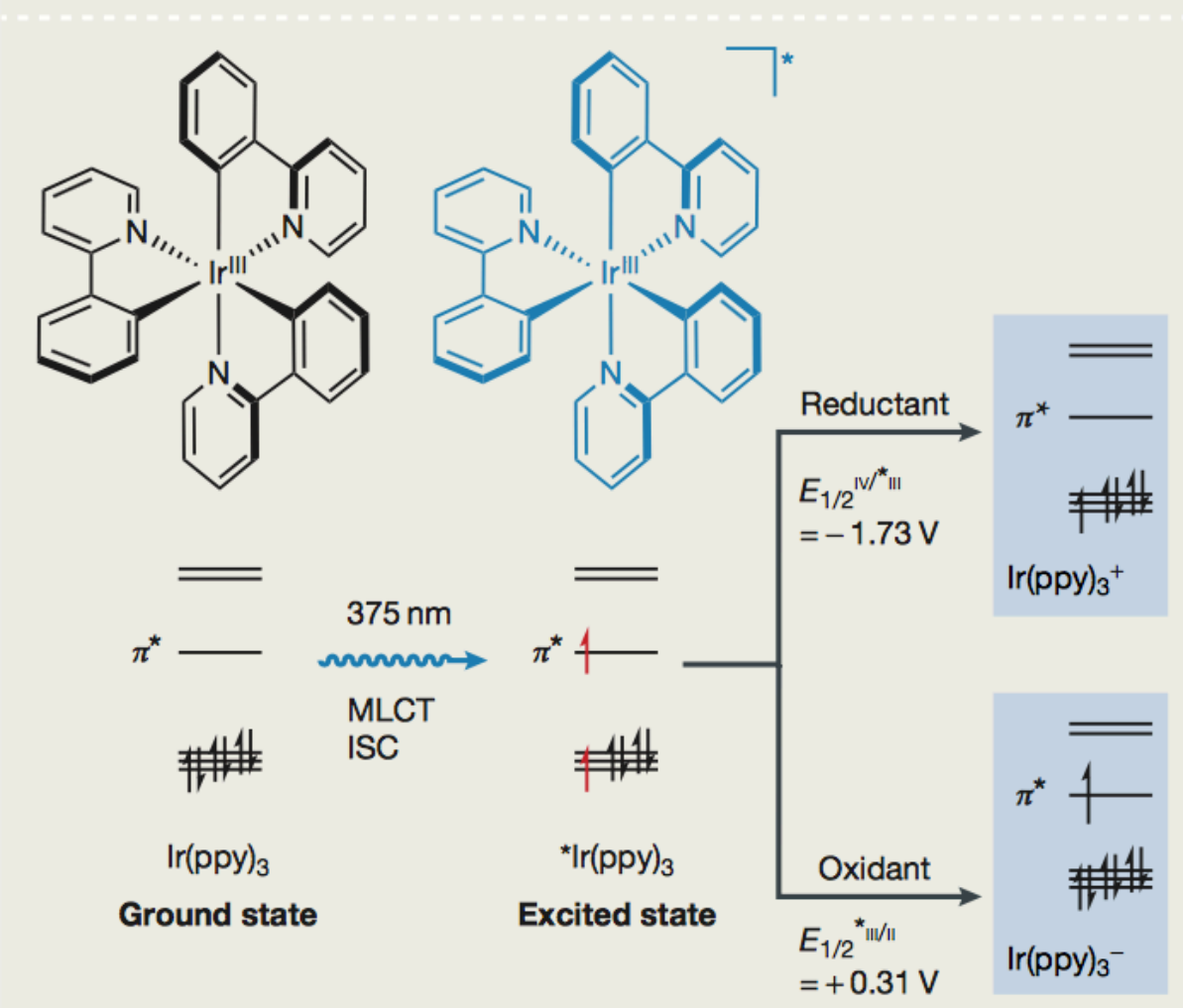

MacMillan, D. W. C. *Nature Rev.* **2017**, *52*,1,

Oxidative and Reductive Quenching Cycle of $[Ru(bpy)_3]^{2+}$

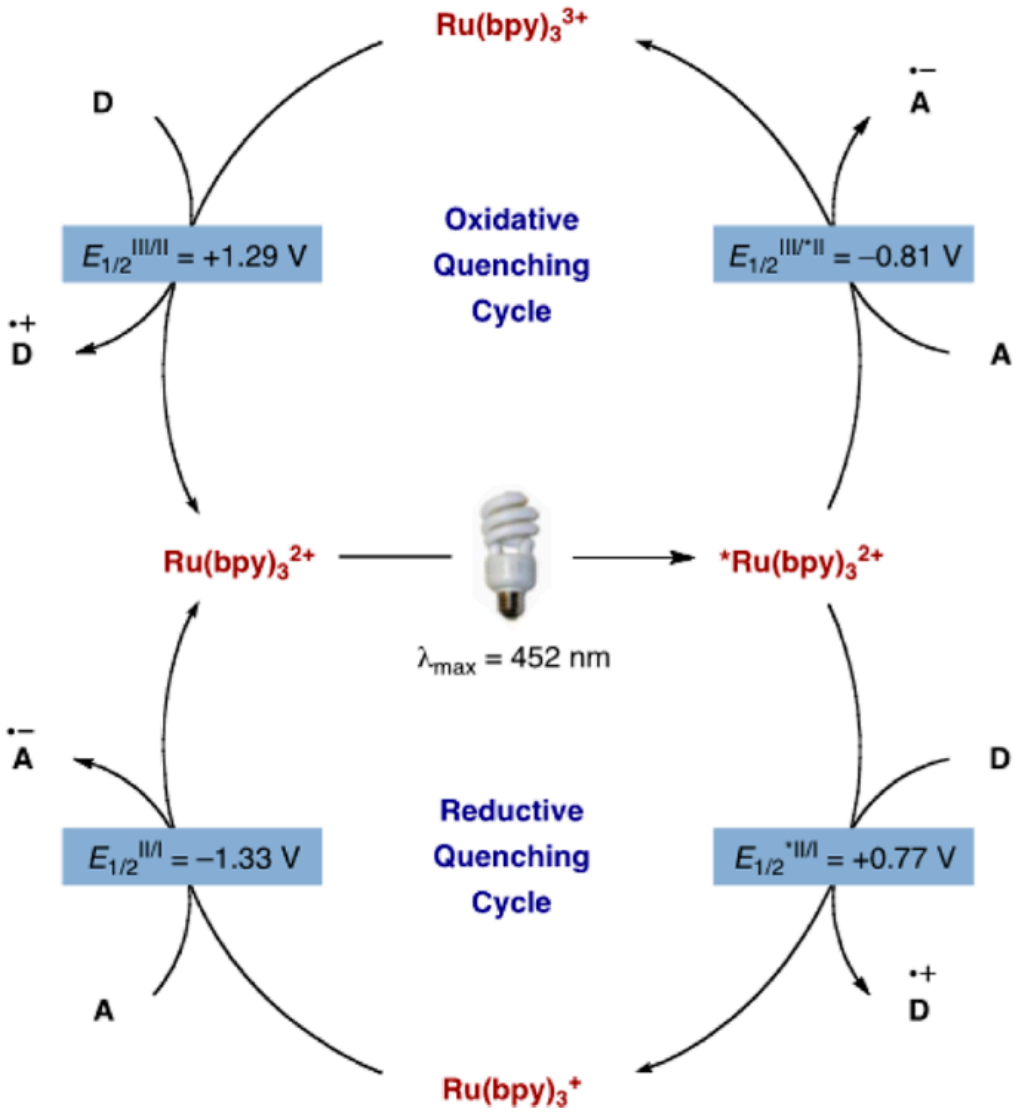

MacMillan, D. W. C. *Chem. Rev.* **2013**, *113*, 5322.